The virus isolated from moose appears to constitute a distinct lineage within species *Orthohepevirus* A, but definitive placement requires a complete genome sequence.

***Orthohepevirus* B.** Although four genotypes of *Orthohepevirus* B have been proposed (Bilic *et al.*, 2009; Hsu & Tsai, 2014; Huang *et al.*, 2004), these are much less diverse than the genotypes of *Orthohepesvirus* A. For example there is <6 % divergence in *Orthohepevirus* B complete genome amino acid sequences (Figs 1 and 3), which is less than the divergence observed within HEV-3 (<9 %) and HEV-4 (<7 %). In addition, the amino acid sequence distances among the eight currently available complete genome sequences of members of species *Orthohepevirus* B form a continuous distribution, where distances within genotypes (maximum 3.3 %) approach those between genotypes (minimum 3.6 %). If additional complete genome sequences were available, this narrow division might disappear.

***Orthohepevirus* C.** The extent of diversity (<11 %) among complete genome amino acid sequences of the rat-derived *Orthohepevirus* C variants barely overlaps that observed among genotypes of species *Orthohepevirus* A (10–18 %). However, much greater divergence is observed between rat and ferret *Orthohepevirus* C variants (23 %). Analysis of the short region of ORF1 for which sequence information is available from additional variants (Fig. 2d) indicates that diversity among greater bandicoot and Asian musk shrew isolates falls within that of the rat variants (Guan *et al.*, 2013; Li *et al.*, 2013), while isolates from the mink group falls within those from ferret (Krog *et al.*, 2013). Based on this information, we propose that *Orthohepevirus* C may be divided into two genotypes, namely HEV-C1, including isolates derived from hosts in the orders Rodentia and Soricomorpha, and HEV-C2, including isolates derived from ferret (and possibly mink).

***Orthohepevirus* D.** A single complete genome sequence is available for species *Orthohepevirus* D, but phylogenetic analysis of a short region of ORF2, for which data from additional isolates are available, suggests a level of diversity equivalent to that within species *Orthohepevirus* A and *Orthohepevirus* C (Fig. 2d). While this is consistent with the existence of multiple genotypes within *Orthohepevirus* D, additional sequence information is required to confirm that these relationships prevail for larger genomic regions.

Subgenotypes

Several studies have attempted to define subgenotypes of genotypes HEV-1, HEV-3 and HEV-4 in the species *Orthohepevirus* A, in some instances based on the analysis of subgenomic regions (Lu *et al.*, 2006; Zhu *et al.*, 2011). Such categories may form useful labels for epidemiological studies (Dai *et al.*, 2013), but more recent analysis of complete genome sequences suggests that it is not possible to define discrete boundaries that distinguish subgenotypes with consistency (Okamoto, 2007; Oliveira-Filho *et al.*, 2013; Smith *et al.*, 2013). We recommend the approach, commonly adopted in several recent publications, of labelling clades apparent within sequence sets (Dai *et al.*, 2013; Ijaz *et al.*, 2014; Oliveira-Filho *et al.*, 2013) without defining them as permanent classification assignments.

Reference sequences and numbering

A recurring difficulty in the literature, relating to molecular studies of members of the family *Hepeviridae,* is that of comparing different studies for which there is no explicit standard sequence with reference to which nucleotides or amino acid residues are numbered. The presence of numerous insertions or deletions and regions of low similarity in alignments of *Hepeviridae* sequences precludes a unified numbering system that is applicable across all species or genera. We recommend that genome sequences be numbered with reference to the first nucleotide of the prototype complete genome sequence available for each species within the genus *Orthohepevirus* (Table 1). Nucleotide sites in variants that contain insertions relative to the prototype sequence should be identified with additional letters, beginning at the site of insertion. For example, a three-nucleotide insertion at position 1788 of the prototype sequence would be numbered 1788a, 1788b, 1788c. Insertions of more than 26 nt would be numbered from the twenty-seventh position as 1788aa, 1788ab, etc. and then as 1788ba, 1788bb, etc. as required. This mirrors the system adopted for HCV (Kuiken *et al.*, 2006). Similarly, amino acid residues should be numbered with reference to the first residue of the appropriate ORF from the reference sequence, for example ORF1-929, with an insertion at this site indicated by suffix letters such as ORF1-929a, ORF1-929b, etc., followed if necessary by ORF1-929 aa, ORF1-929ab, etc.

Conclusions

The proposed classification, which assigns a separate hierarchy of genus and species, respects the different levels of divergence between the cutthroat trout virus and all other hepeviruses. The degrees of sequence divergence and conservation of genomic features associated with these categories closely match those attributed to genera and species in other virus families (e.g. *Picornaviridae, Caliciviridae* and *Flaviviridae*). This description of relationships among members of the family *Hepeviridae* will help to resolve current confusion in the literature and, by providing a rational basis for taxonomic assignments, help to reduce the number of future conflicts as more members of this family are discovered.

METHODS

Phylogenetic analysis included the complete genome sequences in GenBank accessions M73218, M74506, AF082843, FJ906895, AB301710, AJ272108, AB602441, AB856243, AB573435, KJ496143, KJ496144, JN167537, JN167538, GU345042, GU345043, JX120573,

AB847305, AB847306, AB847307, AB847308, AB847309, JN998606, JN998607, AB890001, AB890374, JN597006, JN997392, AM943647, AM943646, GU954430, AY535004, EF206691, KF511797, JQ001749 and HQ731075. Analyses of subgenomic regions included the additional sequences JQ001744-8 and JQ071861 (bat), JN167530-6, KC473527-31, JN040433, KC294199, JF516246, GQ504009-10 and AB725884-900 and AB847310-406 (rat), KF268376-93 (ferret), KC465990-6001 (greater bandicoot and Asian musk rat), KC692369-70 (fox), KC802090-3 (mink), AY043166 (chicken) and KF951328 (moose).

A further dataset included 137 complete genome sequences isolated from humans, pigs, rabbits and wild boar (downloaded from GenBank on 4 February 2014, excluding recombinant sequences and sequences differing from other sequences by less than 0.2 % of nucleotide positions in ORF1), as follows: M73218, AB720034, JF443717, JF443718, JF443720, JF443721, JF443722, JF443723, JF443725, JF443726, JQ655734, FJ457024, D11092, AY204877, AY230202, AF185822, AF076239, X99441, M74506, KC618402, AB780450, AB740232, JQ953664, JQ953665, JQ953666, JN837481, JN906974, AB593690, AB630970, AB630971, AB591733, AB591734, HQ389543, HQ709170, AB481226, AB481228, AB481229, FJ653660, FJ426403, FJ426404, FJ956757, FJ998008, FJ705359, AB291951, AB291953, FJ527832, EU375463, AB189071, AB236320, EU723512, EU723514, AB073912, EU495148, AB089824, AB091394, AB222182, AB222183, AB222184, AB248520, AB248522, AB290312, AB290313, AB291961, AB291962, AB291963, EU723513, EU723516, AB074920, AP003430, EU360977, AB369687, AB369689, AB369691, AB246676, AY575857, AF455784, AY115488, AF060669, KF922359, AF082843, FJ906895, JX109834, AB740220, FJ906896, AB740221, AB740222, JX565469, JQ013791, JQ013792, JQ013793, FJ610232, KC492825, KF176351, JF915746, JQ740781, JX855794, AB291959, JQ655733, JQ655735, JQ655736, AB698654, JQ993308, AB602439, GU361892, GU119960, GU119961, GU206559, HQ634346, AB481227, HM439284, FJ763142, GU188851, AB480825, AB197673, AB197674, AB091395, AB220974, AB291964, AB074915, AB080575, EU676172, AB108537, AB369688, AB369690, EU366959, EF570133, DQ279091, EF077630, AY723745, AB253420, AY594199, AJ272108, AB602441, AB856243, AB573435, KJ496143 and KJ496144. Sequences were aligned using MUSCLE v3.8 (Edgar, 2004) within SSE v1.1 (Simmonds, 2012), and then refined manually. Phylogenetic analysis was conducted using MEGA version 6 (Tamura *et al.*, 2013). Using the optimal model for each dataset, maximum-likelihood trees were reproduced by using the programs Models and Phylogeny in MEGA 6. Distances between nucleotide and amino acid sequences were generated within SSE program. Homology to known protein domains were identified using Motif Scan (http://myhits.isb-sib.ch).

ACKNOWLEDGEMENTS

We are grateful to Dr Patrick Woo for sharing the camel HEV isolate complete genome sequences ahead of general release. This research was supported by a grant from The Wellcome Trust to the Centre for Immunity, Infection and Evolution at the University of Edinburgh. This information is distributed solely for the purpose of pre-dissemination peer review under applicable information quality guidelines. It has not been formally disseminated by the Centers for Disease Control and Prevention/Agency for Toxic Substances and Disease Registry. It does not represent and should not be construed to represent any agency determination or policy. Use of trade names is for identification only and does not imply endorsement by the US Department of Health and Human Services, the Public Health Service, or the Centers for Disease Control and Prevention. The findings and conclusions in this report are those of the authors and do not necessarily represent the views of the Centers for Disease Control and Prevention. The authors declare that they have no conflict of interest.

REFERENCES

Batts, W., Yun, S., Hedrick, R. & Winton, J. (2011). A novel member of the family *Hepeviridae* from cutthroat trout (*Oncorhynchus clarkii*). *Virus Res* **158**, 116–123.

Bilic, I., Jaskulska, B., Basic, A., Morrow, C. J. & Hess, M. (2009). Sequence analysis and comparison of avian hepatitis E viruses from Australia and Europe indicate the existence of different genotypes. *J Gen Virol* **90**, 863–873.

Bodewes, R., van der Giessen, J., Haagmans, B. L., Osterhaus, A. D. M. E. & Smits, S. L. (2013). Identification of multiple novel viruses, including a parvovirus and a hepevirus, in feces of red foxes. *J Virol* **87**, 7758–7764.

Chen, X., Zhang, Q., He, C., Zhang, L., Li, J., Zhang, W., Cao, W., Lv, Y.-G., Liu, Z. & other authors (2012). Recombination and natural selection in hepatitis E virus genotypes. *J Med Virol* **84**, 1396–1407.

Dai, X., Dong, C., Zhou, Z., Liang, J., Dong, M., Yang, Y., Fu, J., Tian, H., Wang, S. & other authors (2013). Hepatitis E virus genotype 4, Nanjing, China, 2001-2011. *Emerg Infect Dis* **19**, 1528–1530.

Drexler, J. F., Seelen, A., Corman, V. M., Fumie Tateno, A., Cottontail, V., Melim Zerbinati, R., Gloza-Rausch, F., Klose, S. M., Adu-Sarkodie, Y. & other authors (2012). Bats worldwide carry hepatitis E virus-related viruses that form a putative novel genus within the family *Hepeviridae*. *J Virol* **86**, 9134–9147.

Edgar, R. C. (2004). MUSCLE: multiple sequence alignment with high accuracy and high throughput. *Nucleic Acids Res* **32**, 1792–1797.

Fan, J. (2009). Open reading frame structure analysis as a novel genotyping tool for hepatitis E virus and the subsequent discovery of an inter-genotype recombinant. *J Gen Virol* **90**, 1353–1358.

Geng, J., Fu, H., Wang, L., Bu, Q., Liu, P., Wang, M., Sui, Y., Wang, X., Zhu, Y. & Zhuang, H. (2011). Phylogenetic analysis of the full genome of rabbit hepatitis E virus (rbHEV) and molecular biologic study on the possibility of cross species transmission of rbHEV. *Infect Genet Evol* **11**, 2020–2025.

Guan, D., Li, W., Su, J., Fang, L., Takeda, N., Wakita, T., Li, T.-C. & Ke, C. (2013). Asian musk shrew as a reservoir of rat hepatitis E virus, China. *Emerg Infect Dis* **19**, 1341–1343.

Hsu, I. W.-Y. & Tsai, H.-J. (2014). Avian hepatitis E virus in chickens, Taiwan, 2013. *Emerg Infect Dis* **20**, 149–151.

Huang, C.-C., Nguyen, D., Fernandez, J., Yun, K. Y., Fry, K. E., Bradley, D. W., Tam, A. W. & Reyes, G. R. (1992). Molecular cloning and sequencing of the Mexico isolate of hepatitis E virus (HEV). *Virology* **191**, 550–558.

Huang, F. F., Sun, Z. F., Emerson, S. U., Purcell, R. H., Shivaprasad, H. L., Pierson, F. W., Toth, T. E. & Meng, X. J. (2004). Determination and analysis of the complete genomic sequence of avian hepatitis E virus (avian HEV) and attempts to infect rhesus monkeys with avian HEV. *J Gen Virol* **85**, 1609–1618.

Ijaz, S., Said, B., Boxall, E., Smit, E., Morgan, D. & Tedder, R. S. (2014). Indigenous hepatitis E in England and Wales from 2003 to 2012: evidence of an emerging novel phylotype of viruses. *J Infect Dis* **209**, 1212–1218.

Johne, R., Heckel, G., Plenge-Bönig, A., Kindler, E., Maresch, C., Reetz, J., Schielke, A. & Ulrich, R. G. (2010a). Novel hepatitis E virus genotype in Norway rats, Germany. *Emerg Infect Dis* **16**, 1452–1455.

Johne, R., Plenge-Bönig, A., Hess, M., Ulrich, R. G., Reetz, J. & Schielke, A. (2010b). Detection of a novel hepatitis E-like virus in

faeces of wild rats using a nested broad-spectrum RT-PCR. *J Gen Virol* **91**, 750–758.

Krog, J. S., Breum, S. Ø., Jensen, T. H. & Larsen, L. E. (2013). Hepatitis E virus variant in farmed mink, Denmark. *Emerg Infect Dis* **19**, 2028–2030.

Kuiken, C., Combet, C., Bukh, J., Shin-I, T., Deleage, G., Mizokami, M., Richardson, R., Sablon, E., Yusim, K. & other authors (2006). A comprehensive system for consistent numbering of HCV sequences, proteins and epitopes. *Hepatology* **44**, 1355–1361.

Lack, J. B., Volk, K. & Van Den Bussche, R. A. (2012). Hepatitis E virus genotype 3 in wild rats, United States. *Emerg Infect Dis* **18**, 1268–1273.

Li, W., Guan, D., Su, J., Takeda, N., Wakita, T., Li, T.-C. & Ke, C. W. (2013). High prevalence of rat hepatitis E virus in wild rats in China. *Vet Microbiol* **165**, 275–280.

Li, T.-C., Yang, T., Ami, Y., Suzaki, Y., Shirakura, M., Kishida, N., Asanuma, H., Takeda, N. & Takaji, W. (2014). Complete genome of hepatitis E virus from laboratory ferrets. *Emerg Infect Dis* **20**, 709–712.

Lin, J., Norder, H., Uhlhorn, H., Belák, S. & Widén, F. (2014). Novel hepatitis E like virus found in Swedish moose. *J Gen Virol* **95**, 557–570.

Lu, L., Li, C. & Hagedorn, C. H. (2006). Phylogenetic analysis of global hepatitis E virus sequences: genetic diversity, subtypes and zoonosis. *Rev Med Virol* **16**, 5–36.

Meng, X.-J. (2013). Zoonotic and foodborne transmission of hepatitis E virus. *Semin Liver Dis* **33**, 41–49.

Ng, T. F. F., Marine, R., Wang, C., Simmonds, P., Kapusinszky, B., Bodhidatta, L., Oderinde, B. S., Wommack, K. E. & Delwart, E. (2012). High variety of known and new RNA and DNA viruses of diverse origins in untreated sewage. *J Virol* **86**, 12161–12175.

Okamoto, H. (2007). Genetic variability and evolution of hepatitis E virus. *Virus Res* **127**, 216–228.

Oliveira-Filho, E. F., König, M. & Thiel, H.-J. (2013). Genetic variability of HEV isolates: inconsistencies of current classification. *Vet Microbiol* **165**, 148–154.

Raj, V. S., Smits, S. L., Pas, S. D., Provacia, L. B. V., Moorman-Roest, H., Osterhaus, A. D. M. E. & Haagmans, B. L. (2012). Novel hepatitis E virus in ferrets, The Netherlands. *Emerg Infect Dis* **18**, 1369–1370.

Reyes, G. R., Purdy, M. A., Kim, J. P., Luk, K. C., Young, L. M., Fry, K. E. & Bradley, D. W. (1990). Isolation of a cDNA from the virus responsible for enterically transmitted non-A, non-B hepatitis. *Science* **247**, 1335–1339.

Simmonds, P. (2012). SSE: a nucleotide and amino acid sequence analysis platform. *BMC Res Notes* **5**, 50.

Simmonds, P., Bukh, J., Combet, C., Deléage, G., Enomoto, N., Feinstone, S., Halfon, P., Inchauspé, G., Kuiken, C. & other authors (2005). Consensus proposals for a unified system of nomenclature of hepatitis C virus genotypes. *Hepatology* **42**, 962–973.

Smith, D. B., Purdy, M. A. & Simmonds, P. (2013). Genetic variability and the classification of hepatitis E virus. *J Virol* **87**, 4161–4169.

Smith, D. B., Bukh, J., Kuiken, C., Muerhoff, A. S., Rice, C. M., Stapleton, J. T. & Simmonds, P. (2014). Expanded classification of hepatitis C virus into 7 genotypes and 67 subtypes: updated criteria and genotype assignment web resource. *Hepatology* **59**, 318–327.

Takahashi, M., Nishizawa, T., Sato, H., Sato, Y., Jirintai, Nagashima, S. & Okamoto, H. (2011). Analysis of the full-length genome of a hepatitis E virus isolate obtained from a wild boar in Japan that is classifiable into a novel genotype. *J Gen Virol* **92**, 902–908.

Takahashi, M., Nishizawa, T., Nagashima, S., Jirintai, S., Kawakami, M., Sonoda, Y., Suzuki, T., Yamamoto, S., Shigemoto, K. & other authors (2014). Molecular characterization of a novel hepatitis E virus (HEV) strain obtained from a wild boar in Japan that is highly divergent from the previously recognized HEV strains. *Virus Res* **180**, 59–69.

Tam, A. W., Smith, M. M., Guerra, M. E., Huang, C.-C., Bradley, D. W., Fry, K. E. & Reyes, G. R. (1991). Hepatitis E virus (HEV): molecular cloning and sequencing of the full-length viral genome. *Virology* **185**, 120–131.

Tamura, K., Stecher, G., Peterson, D., Filipski, A. & Kumar, S. (2013). MEGA6: Molecular Evolutionary Genetics Analysis version 6.0. *Mol Biol Evol* **30**, 2725–2729.

Tsarev, S. A., Emerson, S. U., Reyes, G. R., Tsareva, T. S., Legters, L. J., Malik, I. A., Iqbal, M. & Purcell, R. H. (1992). Characterization of a prototype strain of hepatitis E virus. *Proc Natl Acad Sci U S A* **89**, 559–563.

van Cuyck, H., Fan, J., Robertson, D. L. & Roques, P. (2005). Evidence of recombination between divergent hepatitis E viruses. *J Virol* **79**, 9306–9314.

Wang, H., Zhang, W., Ni, B., Shen, H., Song, Y., Wang, X., Shao, S., Hua, X. & Cui, L. (2010). Recombination analysis reveals a double recombination event in hepatitis E virus. *Virol J* **7**, 129.

Woo, P. C., Lau, S. K., Teng, J. L., Tsang, A. K., Joseph, M., Wong, E. Y., Tang, Y., Sivakumar, S., Xie, J. & other authors (2014). New hepatitis E virus genotype in camels, the Middle East. *Emerg Infect Dis* **20**, 1044–1048.

Zhao, C., Ma, Z., Harrison, T. J., Feng, R., Zhang, C., Qiao, Z., Fan, J., Ma, H., Li, M. & other authors (2009). A novel genotype of hepatitis E virus prevalent among farmed rabbits in China. *J Med Virol* **81**, 1371–1379.

Zhu, Y. M., Dong, S. J., Si, F. S., Yu, R. S., Li, Z., Yu, X. M. & Zou, S. X. (2011). Swine and human hepatitis E virus (HEV) infection in China. *J Clin Virol* **52**, 155–157.

Journal of General Virology (2014), 95, 2166–2175 DOI 10.1099/vir.0.066910-0

Hepatitis E virus egress depends on the exosomal pathway, with secretory exosomes derived from multivesicular bodies

Shigeo Nagashima,[1] Suljid Jirintai,[1] Masaharu Takahashi,[1] Tominari Kobayashi,[1] Tanggis,[1] Tsutomu Nishizawa,[1] Tom Kouki,[2] Takashi Yashiro[2] and Hiroaki Okamoto[1]

Correspondence
Hiroaki Okamoto
hokamoto@jichi.ac.jp

[1]Division of Virology, Department of Infection and Immunity, Jichi Medical University School of Medicine, Tochigi-Ken 329-0498, Japan

[2]Division of Histology and Cell Biology, Department of Anatomy, Jichi Medical University School of Medicine, Tochigi-Ken 329-0498, Japan

Our previous studies indicated that hepatitis E virus (HEV) forms membrane-associated particles in the cytoplasm, most likely by budding into intracellular vesicles, and requires the multivesicular body (MVB) pathway to release virus particles, and the released HEV particles with a lipid membrane retain the *trans*-Golgi network protein 2 on their surface. To examine whether HEV utilizes the exosomal pathway to release the virus particles, we analysed whether the virion release from PLC/PRF/5 cells infected with genotype 3 HEV (strain JE03-1760F) is affected by treatment with bafilomycin A1 or GW4869, or by the introduction of a small interfering RNA (siRNA) against Rab27A or Hrs. The extracellular HEV RNA titre was increased by treatment with bafilomycin A1, but was decreased by treatment with GW4869. The relative levels of virus particles released from cells depleted of Rab27A or Hrs were decreased to 16.1 and 11.5 %, respectively, of that released from cells transfected with negative control siRNA. Electron microscopic observations revealed the presence of membrane-associated virus-like particles with a diameter of approximately 50 nm within the MVB, which possessed internal vesicles in infected cells. Immunoelectron microscopy showed positive immunogold staining for the HEV ORF2 protein on the intraluminal vesicles within the MVB. Additionally, immunofluorescence analysis indicated the triple co-localization of the ORF2, ORF3 and CD63 proteins in the cytoplasm, as specific loculated signals, supporting the presence of membrane-associated HEV particles within the MVB. These findings indicate that membrane-associated HEV particles are released together with internal vesicles through MVBs by the cellular exosomal pathway.

Received 13 April 2014
Accepted 18 June 2014

INTRODUCTION

Hepatitis E virus (HEV), a member of the genus *Hepevirus* in the family *Hepeviridae*, is the causative agent of acute or fulminant hepatitis E, which occurs in many parts of the world, principally as a water-borne infection in developing countries and a zoonotic infection in industrialized countries (Chandra *et al.*, 2008; Colson *et al.*, 2010; Dalton *et al.*, 2008; Purcell & Emerson, 2008; Tei *et al.*, 2003; Yazaki *et al.*, 2003). HEV is a non-enveloped small virus with a diameter of 27–32 nm, present in the bile and faeces of infected hosts. The HEV genome is a positive-sense, ssRNA composed of approximately 7200 nt, which is capped and polyadenylated (Kabrane-Lazizi *et al.*, 1999; Tam *et al.*, 1991). The genome consists of a 5′ UTR, three ORFs (ORF1, ORF2 and ORF3) and a 3′ UTR with a poly(A) tail (Emerson & Purcell, 2007). ORF1 encodes non-structural proteins, including a methyltransferase, a papain-like cysteine protease, a helicase and an RNA-dependent RNA polymerase (Agrawal *et al.*, 2001; Koonin *et al.*, 1992). ORF2 and ORF3 overlap, and their proteins are translated from a bicistronic subgenomic RNA that is 2.2 kb in length (Graff *et al.*, 2006; Ichiyama *et al.*, 2009). The ORF2 protein is the viral capsid protein, while the ORF3 protein is a small protein of only 113 or 114 aa that is thought to act as an adaptor to link the intracellular transduction pathways, reduce the host inflammatory response and protect virus-infected cells (Chandra *et al.*, 2008). Recently, it was found that ORF3 proteins play an important role in virion egress from infected cells (Emerson *et al.*, 2010; Nagashima *et al.*, 2011b; Yamada *et al.*, 2009a).

Four major genotypes (1–4) of HEV have been identified in humans. HEV genotypes 1 and 2 have only been found in humans and are associated with epidemics in developing countries, whereas HEV genotypes 3 and 4 are zoonotic, and are responsible for sporadic or clustered cases of

disease worldwide (Okamoto, 2007). A number of animal strains of HEV have also been identified in increasing numbers of animal species, including chickens, pigs, wild boars, deer, mongooses, rabbits, rats, ferrets and bats (Meng, 2013).

Although HEV particles present in faeces and bile are non-enveloped, those in circulating blood and culture supernatant have been found to be covered with a cellular membrane, similar to enveloped viruses (Takahashi *et al.*, 2008b, 2010; Yamada *et al.*, 2009a). Our previous studies demonstrated that a PASP motif in the ORF3 protein of HEV is necessary for virion release from infected cells (Nagashima *et al.*, 2011b), and that the tumour susceptibility gene 101 (Tsg101) and the enzymic activities of vacuolar protein sorting protein 4 (Vps4A and Vps4B) are involved in the release of HEV virions, indicating that HEV utilizes the multivesicular body (MVB) pathway to release HEV particles, which is promoted by the cellular mechanism of endosomal sorting complexes required for transport (ESCRT) (Nagashima *et al.*, 2011a). Furthermore, it was found that the membrane-associated HEV particles are abundantly present in the lysates of infected cells, thus suggesting that HEV utilizes the MVB machinery intracellularly, but not on the cell surface (Nagashima *et al.*, 2014). Based on the results obtained in such previous studies, it is likely that HEV utilizes the endomembrane for membrane formation and budding. However, the release pathway of the virion has not yet been characterized.

Enveloped viruses, such as hepatitis C virus (HCV), human herpes virus 6 (HHV-6) and rice dwarf virus (RDV), are known to be released from infected cells together with internal vesicles (exosomes) via the cellular exosomal pathway (Mori *et al.*, 2008; Tamai *et al.*, 2012; Wei *et al.*, 2009). Therefore, in the present study, we investigated the requirement of the exosomal pathway for the release of HEV virions by using an inhibitor and accelerator of exosome release or a small interfering RNA (siRNA) against Rab27A, which is a Rab GTPase important for MVB docking at the plasma membrane and exosome secretion (Ostrowski *et al.*, 2010), and Hrs, which is an ESCRT-0 component required for the secretion of exosomes (Tamai *et al.*, 2010). We thereafter observed the membrane-associated virus-like particles in HEV-infected cultured cells by immune electron microscopy.

RESULTS

Requirement of the exosomal pathway for virion release

To investigate the involvement of the exosomal pathway in HEV release, we examined the effects of an accelerator or inhibitor of exosomal release. The accelerator was bafilomycin A1, a vacuolar H^+ ATPase inhibitor, which inhibits lysosomal function (Alvarez-Erviti *et al.*, 2011). We also used GW4869, a neutral sphingomyelinase inhibitor, which is known to inhibit ceramide biosynthesis (Trajkovic *et al.*, 2008). We examined the effects of these agents on the release of HEV in the HEV-infected cells. These drugs had no significant effect on the viability of the cells, as revealed by the 3-(4,5-dimethylthiazol-2-yl)-5-(3-carboxymethoxyphenyl)-2-(4-sulfophenyl)-2H-tetrazolium, inner salt (MTS) assay, within 24 h of the drug application (Fig. 1a). We therefore treated the infected cells with the two drugs for 24 h.

After treatment for 24 h, the cells and their culture supernatants were collected. The extracellular HEV RNA levels were increased to 203.6, 226.8 and 244.9 % of the levels of the DMSO-treated control after treatment with 10, 20 and 50 nM bafilomycin A1, respectively (Fig. 1b, left panel) ($P<0.01$). Conversely, the intracellular HEV RNA levels were reduced to 75.8, 66.7 and 52.1 % of the DMSO control levels after treatment with 10 nM, 20 nM and 50 nM bafilomycin A1, respectively, suggesting that HEV release is greatly facilitated by bafilomycin A1 (Fig. 1b, right panel) ($P<0.01$ or $P<0.001$).

On the other hand, the extracellular HEV RNA levels were reduced to 98.2, 85.6 and 74.0 % of the DMSO control after treatment with 2, 5 and 50 μM GW4869, respectively (Fig. 1c, left panel) ($P<0.001$). In contrast, the intracellular HEV RNA levels were increased to 105.9, 110.7 and 120.6 % of the DMSO control level after treatment with 2, 5 and 50 μM GW4869, respectively (Fig. 1c, right panel) ($P<0.001$). This suggests that GW4869 blocked HEV particle release, without affecting HEV RNA replication, thereby causing the accumulation of HEV particles in the infected cells. These results suggest that the exosomal pathway is required for the release of HEV virions.

Functional involvement of Rab27A and Hrs in virion release

To examine whether the exosomal pathway is functionally involved in HEV release, we utilized siRNA to deplete Rab27A, which is a Rab GTPase required for the secretion of exosomes (Ostrowski *et al.*, 2010), or Hrs, which is known to be necessary for exosome secretion (Tamai *et al.*, 2010), and examined their effects on the HEV virion release from infected cells. Firstly, to confirm the subcellular localization of the ORF3 protein, Rab27A, and Hrs in the PLC/PRF/5 cells inoculated with HEV, we carried out a double immunofluorescent staining assay. The ORF3 protein co-localized with Rab27A (Fig. 2a) and Hrs (Fig. 2b), thus suggesting that both Rab27A and Hrs participate in virus replication.

To deplete Rab27A or Hrs in PLC/PRF/5 cells, the cells were treated with 5 nM siRNA specific for Rab27A (siRab27A) or Hrs (siHrs) or with negative control siRNA (NC siRNA) two days before and four days after virus inoculation (Fig. 2c). Two days after the first transfection of siRNA, the treated cells were inoculated with 1.0×10^5 copies of cell culture-derived HEV. Transfection of siRab27A and siHrs, but not NC siRNA or buffer only (no siRNA), caused a marked reduction in the respective levels of endogenous Rab27A and Hrs in the inoculated cells (Fig. 2d, e; day 0). In contrast, no

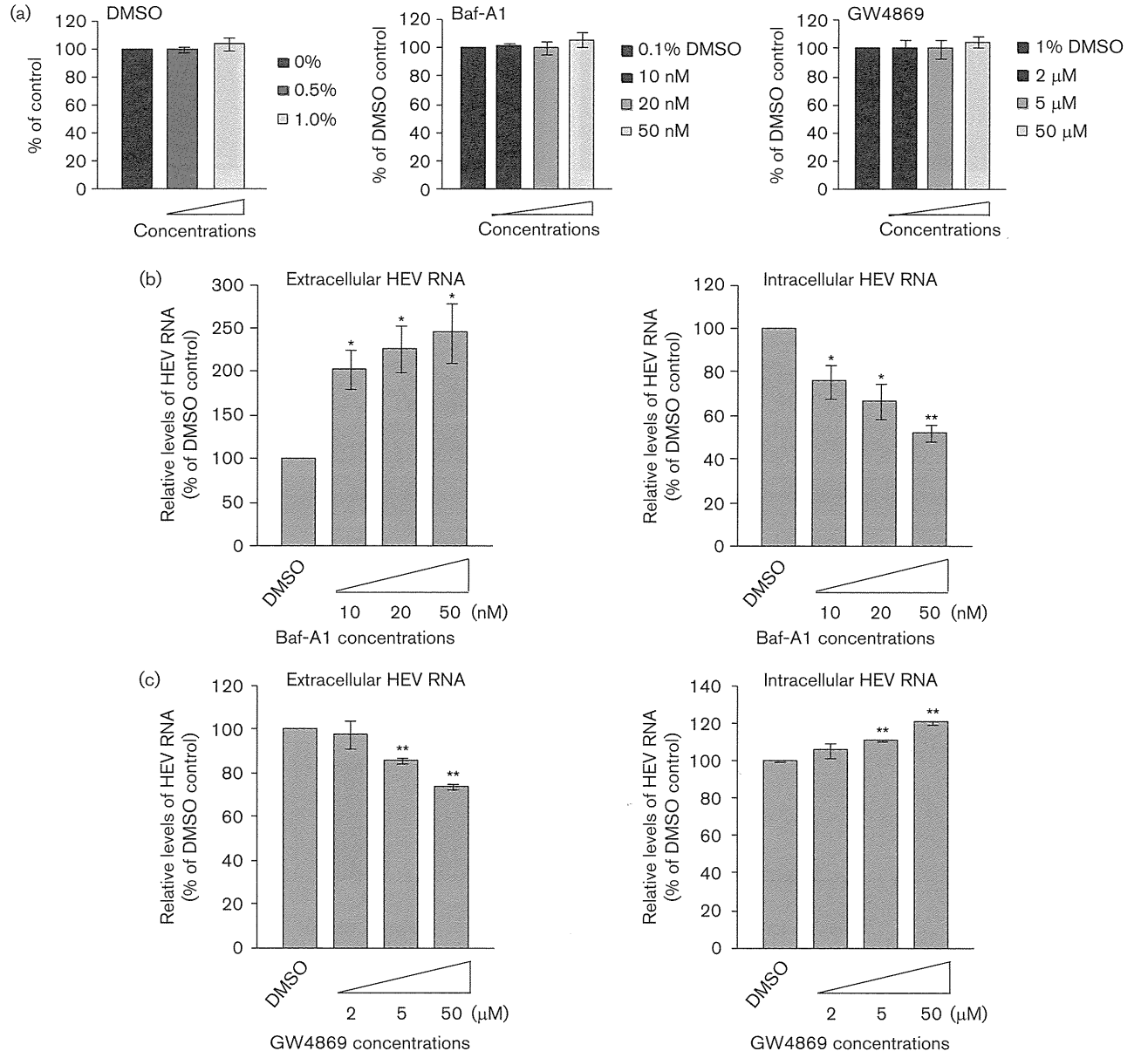

Fig. 1. Effects of drugs on HEV virion release. The PLC/PRF/5 cells infected with culture-produced wild-type HEV (JE03-1760F strain) were cultivated with growth medium containing 0–1.0 % (v/v) DMSO, 0–50 nM bafilomycin A1 (abbreviated as Baf-A1 in this figure) in the presence of 0.1 % DMSO, or 0–50 μM GW4869 in the presence of 1.0 % DMSO for 24 h. (a) The results of an analysis of the cellular proliferation and survival by the MTS assay. (b) The levels of extracellular and intracellular HEV RNA in the infected cells treated with bafilomycin A1. (c) The levels of extracellular and intracellular HEV RNA in the infected cells treated with GW4869. All experiments were done in triplicate, and the data represent the mean ± SD. *, $P<0.01$; **, $P<0.001$.

discernible alteration was observed in the expression level of β-actin. The HEV RNA levels in the culture supernatant of cells transfected with NC siRNA or no siRNA increased gradually from six days post-inoculation, and reached 4.3×10^5 and 4.0×10^5 copies ml^{-1} on day 10, respectively (Fig. 2f). In sharp contrast, the HEV RNA level in the culture supernatant of the siRab27A- or siHrs-transfected cells increased only slightly on day 10, reaching 7.0×10^4 and 5.1×10^4 copies ml^{-1}, respectively ($P<0.001$). The relative levels of virus particles released from cells depleted of Rab27A or Hrs were significantly decreased to 16.1 and 11.5 % of that released from cells transfected with NC siRNA, respectively. The depletion of endogenous Rab27A and Hrs continued at least until day 10, while β-actin was detected at equal levels in both the cells transfected with siRab27A or siHrs and those transfected with NC siRNA or no siRNA.

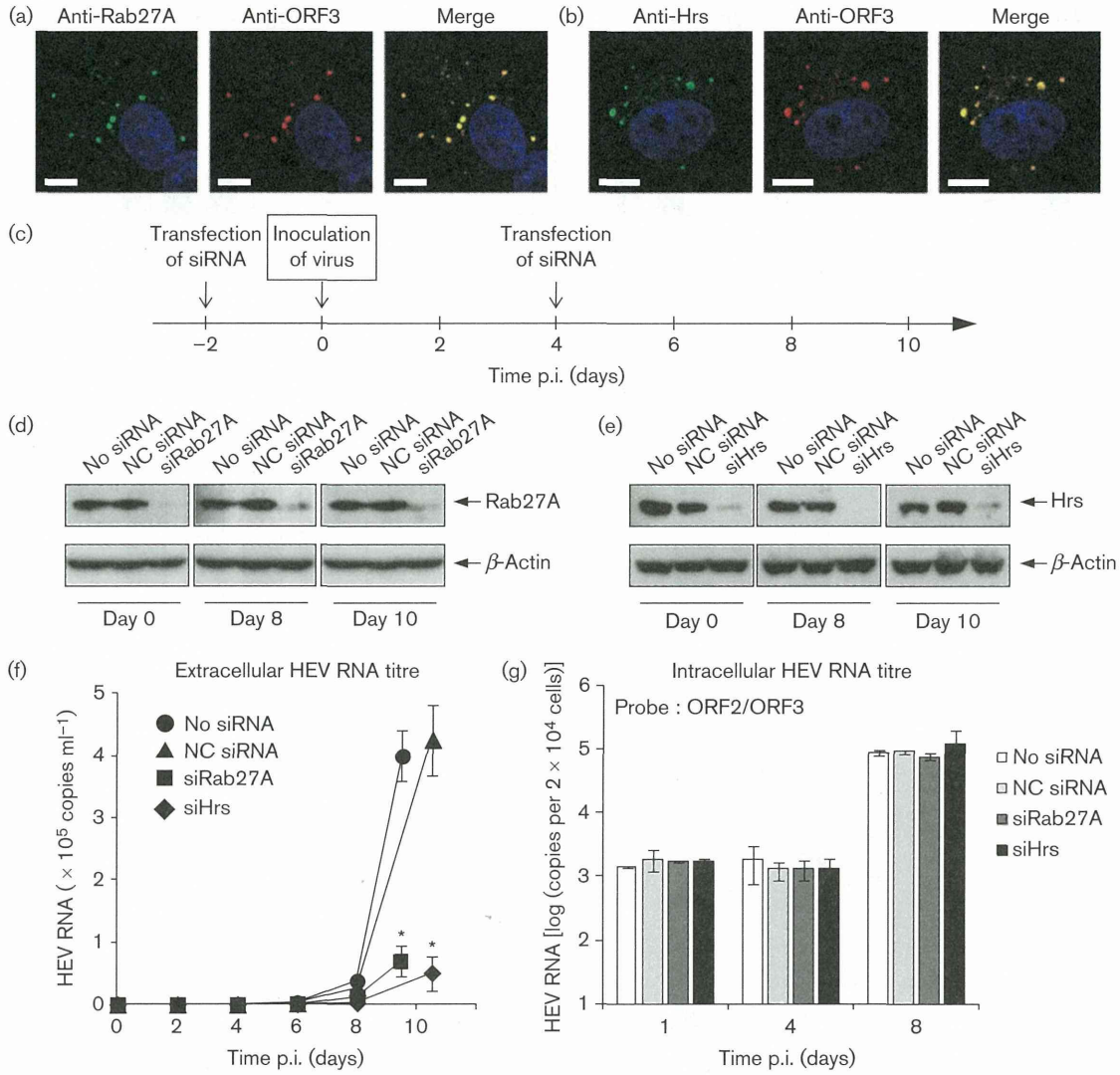

Fig. 2. Effects of siRNAs on HEV virion release. (a, b) Double immunofluorescent staining of the Rab27A (a) or Hrs (b) and ORF3 proteins in PLC/PRF/5 cells infected with cell culture-produced HEV (JE03-1760F strain), as determined by an Alexa Fluor 488-labelled anti-Rab27A (a) or anti-Hrs mAb (b) and an Alexa Fluor 594-labelled anti-ORF3 mAb. Co-localization is shown in yellow. Nuclei were stained with DAPI. All images are representative of two independent experiments. Scale bars, 10 μm. (c) The experimental schedule. PLC/PRF/5 cells were transfected with siRNA two days before and four days after virus inoculation on day 0. Half of the culture medium was replaced with antibiotic-free growth medium every other day after virus inoculation. (d, e) The effects of siRNA specific for Rab27A (d) or Hrs (e). PLC/PRF/5 cells were treated with siRNA specific for Rab27A (siRab27A), Hrs (siHrs), negative control siRNA (NC siRNA) or buffer only (no siRNA). On the indicated days after inoculation, the cells were lysed, and the expression levels of Rab27A (d, upper panel), Hrs (e, upper) and β-actin (d, e, lower panel) were detected by Western blotting analysis using anti-Rab27A, anti-Hrs and anti-β-actin mAbs, respectively. (f) The levels of extracellular HEV RNA in the infected cells treated with siRNA. (g) The levels of intracellular HEV RNA in the infected cells that were transfected with siRNA. The HEV RNA titre was quantified by real-time RT-PCR with primers and a probe targeting the ORF2/ORF3 overlapping region. All experiments were done in triplicate and the data represent the mean ± SD. *, $P<0.001$.

Next, the intracellular viral RNA was serially quantified by real-time reverse transcriptase (RT)-PCR methods with an ORF2/ORF3 probe capable of detecting both genomic and subgenomic RNAs. The HEV RNA levels in the siRab27A- or siHrs-transfected cells were similar to those in the cells transfected with or without control siRNA at one, four and eight days post-inoculation (Fig. 2g), suggesting that the HEV RNA replication was not affected by the siRab27A or siHrs transfection. These results clearly indicated that both Rab27A and Hrs play a pivotal role in the release of HEV virions, and also strongly suggested that HEV utilizes the exosomal pathway to release virions.

Morphological analysis of HEV-infected cells using electron microscopy

To gain further insight into the trafficking patterns of HEV particles in infected cells, we performed an electron microscopic analysis of the HEV-infected cells. First, we analysed the HEV particles released from infected cells using a transmission electron microscope (TEM). Membrane-associated HEV particles were observed extracellularly (Fig. 3a). These particles were approximately 50 nm in diameter and contained the outer membrane and nucleocapsid, which were included in the core exhibiting a high electron density (Fig. 3a). In agreement with previous studies (Balayan *et al.*, 1983; Bradley 1990, Ticehurst 1991), these particles without an outer membrane were estimated to be 30–35 nm in diameter. Furthermore, similar membrane-associated particles were observed extracellularly in HepG2 and A549 cells (Fig. 3b, c). On the other hand, no such virus-like particles were observed in the uninfected cells.

We subsequently examined the intracellular HEV particles using TEM. The MVB, which includes a multitude of small vesicles, were present in the cytoplasm (Fig. 4a), and membrane-associated virus-like particles were found within the MVB (Fig. 4b, c). These virus-like particles possessed the outer membrane and core in the nucleocapsid, and their diameters were consistent with those of the extracellular HEV particles (Fig. 3). Similar virus-like particles were observed in the MVB of HEV-infected HepG2 and A549 cells, but not in the uninfected cells (data not shown).

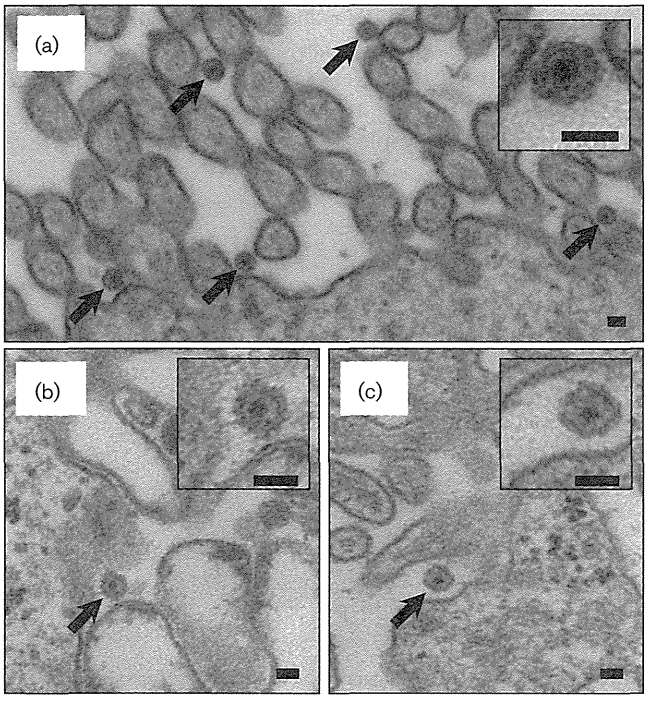

Fig. 3. Electron microscopy findings of the HEV-infected cells. Ultrathin sections of epon-embedded PLC/PRF/5 (a), HepG2 (b) and A549 (c) cells infected with cell culture-produced HEV (JE03-1760F strain). The arrows indicate extracellular membrane-associated virus-like particles. The insets show high magnification images. Scale bars, 50 nm.

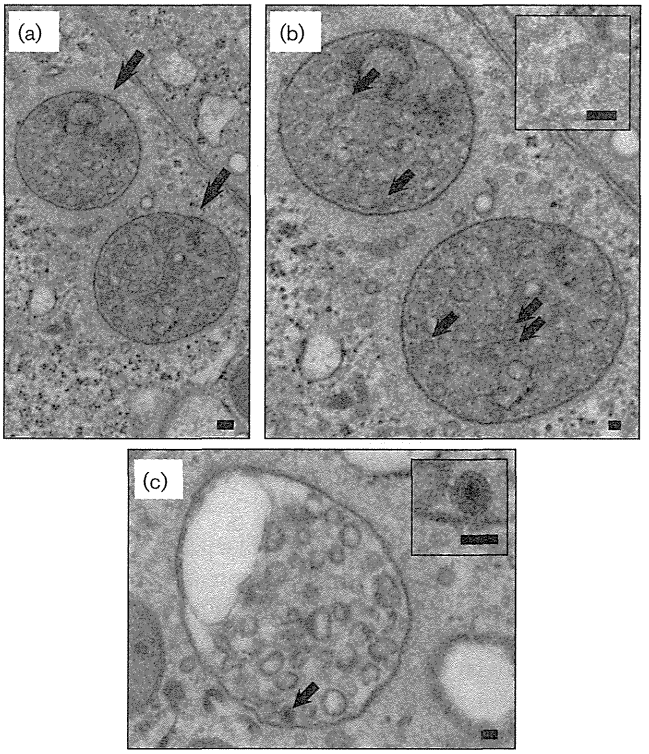

Fig. 4. Morphological features of HEV-infected PLC/PRF/5 cells. In ultrathin sections of epon-embedded cells, the arrows indicate the MVB, including a multitude of small vesicles in the cytoplasm (scale bar, 100 nm) (a) and membrane-associated virus-like particles within the MVB (scale bar, 50 nm) (b, c). The insets show high magnification images.

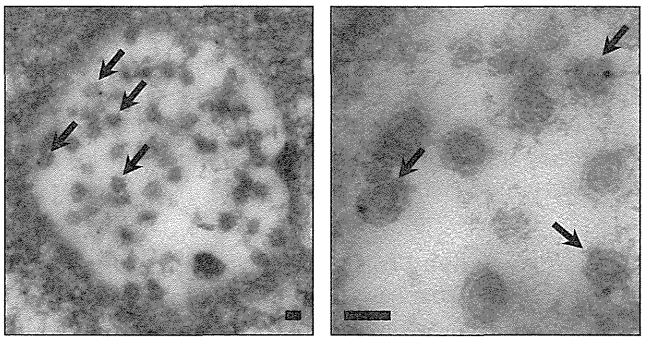

Fig. 5. Immunocytochemical detection of the ORF2 protein within the MVB in HEV-infected PLC/PRF/5 cells. In ultrathin sections of LR white-embedded cells, the arrows indicate positive immunogold staining for the HEV ORF2 protein on the intraluminal vesicles within the MVB. Scale bars, 50 nm.

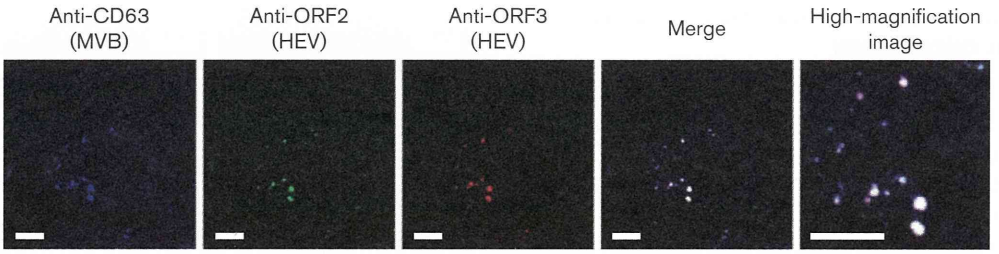

Fig. 6. Results of a triple-labelled immunofluorescence analysis of the ORF2, ORF3 and CD63 proteins in PLC/PRF/5 cells infected with cell culture-produced HEV (JE03-1760F strain). At 20 days post-inoculation, the infected cells were stained simultaneously with Alexa Fluor 350-conjugated anti-CD63, Alexa Fluor 488-conjugated anti-ORF2 and Alexa Fluor 594-conjugated anti-ORF3 antibodies. Triple localization is shown in white. All images are representative of two independent experiments. Scale bars, 10 μm.

Next, to confirm whether the virus-like particles were those of HEV, we carried out immunoelectron microscopy studies using a mouse mAb against the ORF2 protein of HEV (H6225) and immunogold-conjugated anti-mouse IgG (12 nm colloidal gold). Positive immunogold staining for the HEV ORF2 protein was detectable on the intraluminal vesicles within the MVB (Fig. 5). In contrast, no specific binding of gold colloid was observed in the cells that reacted only with immunogold-conjugated anti-mouse IgG. These findings indicate that membrane-associated HEV particles are present within MVBs, together with internal vesicles.

Co-localization of the virus proteins (ORF2 and ORF3) with CD63

In previous studies, we demonstrated that the ORF3 protein is present on the surface of membrane-associated HEV particles in the circulation and in the culture supernatants (Takahashi *et al.*, 2008b, 2010), and that it is co-localized with CD63, one of the MVB marker proteins, in the cytoplasm of the infected cells (Nagashima *et al.*, 2011a). To examine the intracellular co-localization of the three proteins (ORF2, ORF3 and CD63), PLC/PRF/5 cells inoculated with HEV were fixed and stained simultaneously with Alexa Fluor 350-conjugated anti-CD63, Alexa Fluor 488-conjugated anti-ORF2 and Alexa Fluor 594-conjugated anti-ORF3 antibodies. These proteins partially co-localized in the cytoplasm and exhibited specific loculated signals (Fig. 6), supporting the observation that membrane-associated HEV particles are present within the MVB.

Exosomes derived from HEV-infected cells contain viral proteins

To establish the role of exosomes in secretion of HEV particles from infected cells, exosomes were isolated from culture supernatants of HEV-infected or -uninfected PLC/PRF/5 cells using differential centrifugation. As shown in Fig. 7 (upper panel), Western blot analysis of exosomes confirmed the presence of CD81, one of exosome marker proteins (Escola *et al.*, 1998), in both cells. Moreover, exosomes isolated from HEV-infected cells contained detectable levels of viral ORF2 and ORF3 proteins (Fig. 7, middle and lower panels). These results support the hypothesis that secretion of HEV particles is associated with exosomes.

DISCUSSION

Many enveloped viruses are known to complete their replication cycle by budding from the plasma membrane (Demirov *et al.*, 2002; Hartlieb & Weissenhorn, 2006; Jayakar *et al.*, 2004). Human immunodeficiency virus, Ebola virus and other RNA viruses utilize the ESCRT mechanism to promote their escape from host cells by redirecting ESCRT complexes to the cell surface, where they

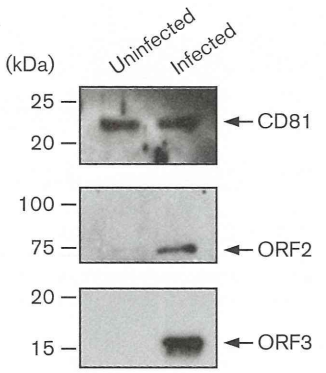

Fig. 7. Western blot analysis of the purified exosomes from the culture supernatants of HEV-infected or -uninfected PLC/PRF/5 cells. The cells were incubated in serum-free medium, and the exosomes were purified from the culture supernatants by differential centrifugation. Exosomes were subjected to Western blot analysis with an anti-CD81 antibody (upper panel). ORF2 or ORF3 proteins were detected by Western blot analysis with the anti-ORF2 mAb (middle panel) or the anti-ORF3 mAb (lower panel), respectively. Molecular markers are indicated in kDa.

appear to drive the budding and fission of the viral particles (Demirov *et al.*, 2002; Garrus *et al.*, 2001; Martin-Serrano *et al.*, 2003). On the other hand, in most herpesviruses, the final envelopment occurs in the Golgi or post-Golgi compartments, such as the *trans*-Golgi network (TGN), or endosomes (Crump *et al.*, 2007, Fraile-Ramos *et al.*, 2007). It has been reported that HHV-6 buds at TGN-associated membranes, which express CD63 and TGN46, and that CD63 is incorporated into the virions (Mori *et al.*, 2008). In addition, the virions are released together with internal vesicles (exosomes) through the MVBs via the cellular exosomal pathway. Similarly, RDV particles are released, together with small vesicles similar to secreted vesicles (exosomes), from infected cells (Wei *et al.*, 2009).

It has recently been reported that the Hrs-dependent exosomal pathway plays an important role in HCV secretion (Tamai *et al.*, 2012). Our previous study revealed that the membrane-associated HEV particles are abundantly present in the lysates of infected cells and the *trans*-Golgi network protein 2 derived from the TGN is retained on the surface of the particles (Nagashima *et al.*, 2014). This suggests that the membrane of membrane-associated HEV particles is derived from the intracellular membrane, not from the cell surface. In the present study, we confirmed the previous observations regarding the origin of the membrane of membrane-associated HEV virions, and demonstrated that HEV utilizes the exosomal pathway to shed from the infected cells.

As expected, in the present study, the virion release was increased by treatment with bafilomycin A1, which is known to act as an accelerator of exosome release due to lysosomal inhibition (Alvarez-Erviti *et al.*, 2011). In contrast, the virion release was decreased by treatment with GW4869, which was reported to act as a blocker of exosome release by inhibiting ceramide biosynthesis (Kosaka *et al.*, 2010; Trajkovic *et al.*, 2008) (Fig. 1b, c). When siRNA against Rab27A or Hrs was introduced, the relative levels of virus particles released from the cells depleted of Rab27A or Hrs decreased significantly (Fig. 2d, e). These results are in agreement with our proposal that HEV utilizes the exosomal pathway to release virions, similar to that observed for known enveloped viruses, such as HCV, HHV-6 and RDV (Tamai *et al.*, 2012; Mori *et al.*, 2008; Wei *et al.*, 2009).

Our previous study demonstrated that HEV recruits Tsg101 via its PSAP motif in the ORF3 protein, that it requires the late domain function for virion release from infected cells and that the enzymic activity of Vps4 is involved in the virus release (Nagashima *et al.*, 2011a). These results suggest that, although HEV is known to be a non-enveloped virus, it requires the MVB pathway for its release from infected cells. However, it remains unknown whether HEV buds from the membrane of the MVB or other endosomes. In this study, an electron microscopic observation revealed that the membrane-associated HEV particles were present within the MVB, together with internal vesicles (Fig. 4). In support of this observation, the specific binding of antibodies with gold colloid for the HEV ORF2 protein was observed on the intraluminal vesicles within the MVB (Fig. 5), although aggregated forms of gold colloid were not observed in the MVB, probably due to the attenuation of the antigenicity of the ORF2 protein during the fixation of cells for microscopic observation. These results indicate that HEV obtains a membrane on the surface due to the budding of the MVB membrane.

We have previously reported that HEV particles present in the circulating blood and culture supernatants are associated with a cellular membrane and the ORF3 protein (Takahashi *et al.*, 2010). The membrane association of virions in serum and culture supernatants was also noted for rat HEV obtained from wild rats (*Rattus rattus*) (Jirintai *et al.*, 2014), which may be a characteristic common to hepeviruses. In this study, we revealed the presence of the membrane on the surface of HEV particles by using TEM (Fig. 3). The diameter of these membrane-associated particles was estimated to be approximately 50 nm, and due to the thickness of the membrane (8–10 nm), the diameter of the HEV particles without the lipid membrane was estimated to be 30–35 nm, similar to the known HEV particles previously evaluated in faeces and bile (Balayan *et al.*, 1983; Bradley, 1990; Ticehurst, 1991).

Recently, Ramakrishnaiah *et al.* (2013) reported that hepatic exosomes can transmit productive HCV infection *in vitro*, and are partially resistant to antibody neutralization. Similarly, hepatitis A virus particles released from cells are cloaked in host-derived membranes, thereby protecting the virion from antibody-mediated neutralization (Feng *et al.*, 2013). Furthermore, these enveloped viruses resemble exosomes. Recent evidence indicates that virus spread to secondary sites is not achieved only by lytic mechanisms, and a non-lytic cell–cell strategy has been suggested for coxsackievirus B3 (Inal & Jorfi, 2013). A physical interaction between infected and non-infected cells is thought to be related to the extracellular vesicles (exosome). In HEV, we reported that immune sera have no ability to neutralize the membrane-associated HEV particles in serum and culture supernatants (Takahashi *et al.*, 2010). In this study, we revealed that membrane-associated HEV particles are released together with internal vesicles (exosomes) through MVBs by the cellular exosomal pathway. The membrane structure of membrane-associated particles closely resembles that of exosomes. It is likely that the membrane-associated HEV particles play a part in cell-to-cell transmission, and that exosomes transmit productive HEV infection.

In conclusion, this present study revealed that the membrane-associated HEV particles are present in the MVB with internal vesicles, and that HEV virion release is related to the exosomal pathway, thus indicating that HEV egress depends on the exosomal pathway with secretory internal vesicles (exosomes) through the MVBs. Further studies on viral particles and

cellular exosomes are warranted to elucidate the effects of their production on the viral pathogenesis and the virus entry factors required for infection.

METHODS

Cell culture. PLC/PRF/5 (ATCC no. CRL-8024; American Tissue Culture Collection), HepG2 (No. RCB0459; RIKEN BRC Cell Bank) and A549 (No. RCB0098; RIKEN BRC Cell Bank) cells were grown in Dulbecco's modified Eagle medium (DMEM; Invitrogen) supplemented with 10 % (v/v) heat-inactivated FBS (HANA-NESCO BIO), 100 U penicillin ml^{-1}, 100 μg streptomycin ml^{-1} and 2.5 μg amphotericin B ml^{-1} (growth medium) at 37 °C in a humidified 5 % CO_2 atmosphere, as described previously (Tanaka *et al.*, 2007).

Viruses. A culture supernatant containing a cell culture-adapted JE03-1760F strain (passage 26 : 4.3×10^7 copies ml^{-1}) (Lorenzo *et al.*, 2008) was used for virus inoculation.

Virus inoculation. Monolayers of PLC/PRF/5, HepG2 and A549 cells in six-well plates (IWAKI) were inoculated at 1.0×10^6 copies of HEV progenies diluted with PBS without Mg^{2+} and Ca^{2+} [PBS(−)], containing 0.2 % (w/v) BSA (Sigma-Aldrich). After inoculation at room temperature for 1 h, the cells were washed with PBS(−), 0.5 ml growth medium was added to each well and the cells were incubated at 35.5 °C. To analyse the effects of drug treatment, infected PLC/PRF/5 cells were washed with PBS(−), trypsinized and collected by centrifugation at 100 *g* at room temperature for 5 min. After removal of the supernatant, the cell pellet was resuspended in growth medium and the cells were plated onto new 24-well plates (BD Falcon).

MTS assay. Monolayers of PLC/PRF/5 cells in 96-well plates (IWAKI) were incubated with growth medium containing the indicated concentrations of bafilomycin A1 (AdipoGen), GW4869 (Sigma-Aldrich) or DMSO (Nacalai Tesque) at 37 °C (see Fig. 1a). After 24 h of incubation, the number of viable cells was measured by the MTS assay using a CellTiter 96 Aqueous One Solution Cell Proliferation Assay (Promega) according to the manufacturer's recommendations.

Treatment of PLC/PRF/5 cells with drugs during HEV infection. Monolayers of HEV-infected PLC/PRF/5 cells grown in 24-well plates were washed with PBS(−) and incubated with the indicated concentrations of bafilomycin A1 or GW4869 in growth medium containing 0.1 and 1 % (v/v) DMSO, respectively (see Fig. 1b, c). After 24 h of incubation, the culture supernatant was collected and centrifuged at 1300 *g* at room temperature for 2 min, and the supernatant was stored at −80 °C until use. The cells were washed and then collected in the presence of TRIzol reagent (Invitrogen). The samples were stored at −80 °C until use.

Quantification of HEV RNA. RNA extraction from the culture supernatants was performed using the TRIzol-LS reagent (Invitrogen). Intracellular RNA was extracted from cultured cells using the TRIzol reagent. The quantification of HEV RNA was performed by real-time RT-PCR using a LightCycler apparatus (Roche), with a QuantiTect Probe RT-PCR kit (Qiagen) and two sets of primers and a probe targeting the ORF2 and ORF3 overlapping region, as described previously (Takahashi *et al.*, 2008a).

Immunofluorescence assay. To stain the HEV-infected PLC/PRF/5 cells in a four-well chamber slide (Nunc), mAbs against the ORF2 protein (anti-ORF2 mAb; H6225) (Takahashi *et al.*, 2008a) and ORF3 protein (anti-ORF3 mAb; TA0536) (Takahashi *et al.*, 2008b) were used to label cells by using the Zenon Alexa Fluor 488-mouse IgG_1 and Zenon Alexa Fluor 594-mouse IgG_{2a} labelling kits (Molecular Probes), respectively, according to the manufacturer's instructions. Similarly, mouse anti-Rab27A (SAB1404290; Sigma-Aldrich) and anti-Hrs (WH0009146M1; Sigma-Aldrich) mAbs and a rabbit anti-CD63 polyclonal antibody (H-193; Santa Cruz Biotechnology) were labelled using the Zenon Alexa Fluor 488-mouse IgG_1 and Zenon Alexa Fluor 350-rabbit IgG labelling kits (Molecular Probes), respectively.

Briefly, the cultured cells were fixed in 4 % (v/v) paraformaldehyde (Wako Pure Chemical Industries) at room temperature for 15 min and treated with 50 mM glycine in PBS(−) at room temperature for 30 min. The cells were then treated with cold methanol at −20 °C for 15 min and permeabilized in PBS containing 0.2 % (v/v) Triton X-100 at room temperature for 15 min. Non-specific binding was blocked with 1 % BSA in PBS(−) at room temperature for 30 min. Zenon labelled complexes were diluted to 1 : 50 for all primary antibodies in PBS(−) containing 1 % (w/v) BSA, and were applied to the cells at room temperature for 1 h. The nuclei were counterstained with DAPI (Roche). The slide glasses were mounted with Fluoromount/Plus (Diagnostic BioSystems) and then viewed under a FV1000 confocal laser microscope (Olympus). All images are representative of two independent experiments.

RNA interference. The following siRNAs were obtained from Dharmacon, and were used in the present study: human Rab27A (siGENOME SMARTpool M-004667-00-0005), human Hrs (siGENOME SMARTpool M-016835-00-0005) and control siRNA (siGENOME Non-Targeting siRNA Pool no.1 D-001206-13-05). The PLC/PRF/5 cells were seeded at a density of 1.0×10^5 cells per well in 24-well plates in antibiotic-free growth medium. The cells were transfected with 5 nM (final concentration) siRNA in Opti-MEM (Gibco/Invitrogen) using DharmaFECT 1 (Dharmacon) according to the manufacturer's instructions, two days before and four days after virus inoculation.

Virus inoculation. Monolayers of PLC/PRF/5 cells in 24-well plates, which were pretreated with siRNA against Rab27A or Hrs as described above, were inoculated with 1.0×10^5 copies of HEV progenies in the culture supernatant of JE03-1760F-infected cells. After incubation at room temperature for 1 h, the cells transfected with siRNA were washed with PBS(−), and 0.5 ml of antibiotic-free growth medium was added to each well, and the cells were incubated at 37 °C. Every other day, half of the culture medium (0.25 ml) of the siRNA-transfected cells was replaced with antibiotic-free growth medium. The collected culture medium was centrifuged at 1300 *g* at room temperature for 2 min, and the supernatant was stored at −80 °C until use.

Western blot analysis. The siRNA-transfected cells were lysed in lysis buffer [50 mM Tris/HCl (pH 8.0), 1 % (v/v) NP-40, 150 mM NaCl and protease inhibitor cocktail (Sigma-Aldrich)], and the proteins in the cell lysates were separated by SDS-PAGE. The proteins were blotted onto PVDF membranes (0.45 μm; Millipore), immunodetected with an anti-Rab27A, anti-Hrs or anti-β-actin (Sigma-Aldrich) mAb and then visualized by chemiluminescence using the ImageQuant LAS500 (GE Healthcare), as described previously (Yamada *et al.*, 2009b). Similarly, exosomes isolated from culture supernatants were subjected to SDS-PAGE and immunodetected with a rabbit anti-CD81 polyclonal antibody (System Biosciences). Viral proteins were detected by mAbs against the ORF2 protein (anti-ORF2 mAb; H6210) (Takahashi *et al.*, 2008a) or ORF3 protein (anti-ORF3 mAb; TA0536).

Electron microscopy. The uninfected cultured cells and cells infected with strain JE03-1760F were scraped off the six-well plates and pelleted by centrifugation at 300 *g* at room temperature for 3 min. Small pieces of cells were fixed with 2.5 % (v/v) glutaraldehyde in sodium phosphate buffer (0.1 M, pH 7.4) for 1.5 h at 4 °C, and were post-fixed with 1 % (v/v) OsO_4 in sodium phosphate buffer (0.2 M, pH 7.4) for 1.5 h at 4 °C. After dehydration with a series of

increasing concentrations of ethanol, the specimens were embedded in an epoxy resin mixture. Ultrathin sections were cut using an ultramicrotome (NACC), stained with aqueous uranyl acetate and lead citrate (Reynolds, 1963) and examined using a TEM (model HT-7600; Hitachi) at an acceleration voltage of 80 kV.

Immunoelectron microscopy. For immunoelectron microscopy, small pieces of cultured cells that were or were not infected with strain JE03-1760F were fixed with 2.5 % glutaraldehyde in sodium phosphate buffer (0.1 M, pH 7.4) for 1.5 h at 4 °C. After dehydration with a series of increasing concentrations of ethanol, the specimens were embedded in LR white (London Resin Company). Ultrathin sections were cut and mounted on a nickel grid supported by a Formvar film. The ultrathin sections on the grid were treated with 10 % Blocker BSA (Thermo Scientific) in PBS at room temperature for 20 min to block non-specific reactions. The sections were reacted with anti-ORF2 mAb at room temperature for 18 h, the sections were then washed with PBS and reacted with a secondary antibody (12 nm Colloidal Gold-AffiniPure goat anti-mouse IgG; Jackson ImmunoResearch) for 2 h at room temperature, and washed again with PBS. The immunostained sections were stained with aqueous uranyl acetate and observed by a TEM, as described above.

Isolation of exosomes. Exosomes from cell culture supernatants were isolated by differential centrifugation as described (Ostrowski *et al.*, 2010) with several modifications. In brief, HEV-infected or -uninfected PLC/PRF/5 cells were replaced by serum-free medium (VP-SFM, Gibco/Invitrogen) and then cultured for 48 h. The collected culture supernatants were centrifuged at 1200 ***g*** for 10 min, and at 10 000 ***g*** for 30 min at 4 °C to remove cells and debris. The second supernatants were sequentially centrifuged at 100 000 ***g*** for 60 min at 4 °C, using an SW40 rotor (Beckman Coulter Instruments). The exosome pellet was resuspended in PBS(−) and then subjected to SDS-PAGE and Western blot analysis as described above.

Statistical analysis. The results were presented as the mean ± SD. Statistical significance was assessed by Student's *t*-test. *P*-values of less than 0.05 were considered significant.

ACKNOWLEDGEMENTS

This work was supported in part by Grants-in-Aid for Young Scientists (B) from the Japan Society for the Promotion of Science (JSPS) to S. N. (grant number: 25860343), and grants to H. O. from the Ministry of Health, Labour and Welfare of Japan (H24-Hepatitis-General-002) and MEXT-Supported Program for the Strategic Research Foundation at Private Universities, 2013-2017 (S1311030).

REFERENCES

Agrawal, S., Gupta, D. & Panda, S. K. (2001). The 3′ end of hepatitis E virus (HEV) genome binds specifically to the viral RNA-dependent RNA polymerase (RdRp). *Virology* **282**, 87–101.

Alvarez-Erviti, L., Seow, Y., Schapira, A. H., Gardiner, C., Sargent, I. L., Wood, M. J. & Cooper, J. M. (2011). Lysosomal dysfunction increases exosome-mediated alpha-synuclein release and transmission. *Neurobiol Dis* **42**, 360–367.

Balayan, M. S., Andjaparidze, A. G., Savinskaya, S. S., Ketiladze, E. S., Braginsky, D. M., Savinov, A. P. & Poleschuk, V. F. (1983). Evidence for a virus in non-A, non-B hepatitis transmitted via the fecal-oral route. *Intervirology* **20**, 23–31.

Bradley, D. W. (1990). Enterically-transmitted non-A, non-B hepatitis. *Br Med Bull* **46**, 442–461.

Chandra, V., Taneja, S., Kalia, M. & Jameel, S. (2008). Molecular biology and pathogenesis of hepatitis E virus. *J Biosci* **33**, 451–464.

Colson, P., Borentain, P., Queyriaux, B., Kaba, M., Moal, V., Gallian, P., Heyries, L., Raoult, D. & Gerolami, R. (2010). Pig liver sausage as a source of hepatitis E virus transmission to humans. *J Infect Dis* **202**, 825–834.

Crump, C. M., Yates, C. & Minson, T. (2007). Herpes simplex virus type 1 cytoplasmic envelopment requires functional Vps4. *J Virol* **81**, 7380–7387.

Dalton, H. R., Bendall, R., Ijaz, S. & Banks, M. (2008). Hepatitis E: an emerging infection in developed countries. *Lancet Infect Dis* **8**, 698–709.

Demirov, D. G., Ono, A., Orenstein, J. M. & Freed, E. O. (2002). Overexpression of the N-terminal domain of TSG101 inhibits HIV-1 budding by blocking late domain function. *Proc Natl Acad Sci U S A* **99**, 955–960.

Emerson, S. U. & Purcell, R. H. (2007). Hepatitis E virus. In *Fields Virology*, 5th edn, pp. 3047–3058. Edited by D. M. Knipe, P. M. Howley, D. E. Griffin, R. A. Lamb, M. A. Martin, B. Roizman & S. E. Straus. Philadelphia: Lippincott Williams & Wilkins.

Emerson, S. U., Nguyen, H. T., Torian, U., Burke, D., Engle, R. & Purcell, R. H. (2010). Release of genotype 1 hepatitis E virus from cultured hepatoma and polarized intestinal cells depends on open reading frame 3 protein and requires an intact PXXP motif. *J Virol* **84**, 9059–9069.

Escola, J. M., Kleijmeer, M. J., Stoorvogel, W., Griffith, J. M., Yoshie, O. & Geuze, H. J. (1998). Selective enrichment of tetraspan proteins on the internal vesicles of multivesicular endosomes and on exosomes secreted by human B-lymphocytes. *J Biol Chem* **273**, 20121–20127.

Feng, Z., Hensley, L., McKnight, K. L., Hu, F., Madden, V., Ping, L., Jeong, S. H., Walker, C., Lanford, R. E. & Lemon, S. M. (2013). A pathogenic picornavirus acquires an envelope by hijacking cellular membranes. *Nature* **496**, 367–371.

Fraile-Ramos, A., Pelchen-Matthews, A., Risco, C., Rejas, M. T., Emery, V. C., Hassan-Walker, A. F., Esteban, M. & Marsh, M. (2007). The ESCRT machinery is not required for human cytomegalovirus envelopment. *Cell Microbiol* **9**, 2955–2967.

Garrus, J. E., von Schwedler, U. K., Pornillos, O. W., Morham, S. G., Zavitz, K. H., Wang, H. E., Wettstein, D. A., Stray, K. M., Côté, M. & other authors (2001). Tsg101 and the vacuolar protein sorting pathway are essential for HIV-1 budding. *Cell* **107**, 55–65.

Graff, J., Torian, U., Nguyen, H. & Emerson, S. U. (2006). A bicistronic subgenomic mRNA encodes both the ORF2 and ORF3 proteins of hepatitis E virus. *J Virol* **80**, 5919–5926.

Hartlieb, B. & Weissenhorn, W. (2006). Filovirus assembly and budding. *Virology* **344**, 64–70.

Ichiyama, K., Yamada, K., Tanaka, T., Nagashima, S., Jirintai, Takahashi, M. & Okamoto, H. (2009). Determination of the 5′-terminal sequence of subgenomic RNA of hepatitis E virus strains in cultured cells. *Arch Virol* **154**, 1945–1951.

Inal, J. M. & Jorfi, S. (2013). Coxsackievirus B transmission and possible new roles for extracellular vesicles. *Biochem Soc Trans* **41**, 299–302.

Jayakar, H. R., Jeetendra, E. & Whitt, M. A. (2004). Rhabdovirus assembly and budding. *Virus Res* **106**, 117–132.

Jirintai, S., Tanggis, Mulyanto, Suparyatmo, J. B., Takahashi, M., Kobayashi, T., Nagashima, S., Nishizawa, T. & Okamoto, H. (2014). Rat hepatitis E virus derived from wild rats (*Rattus rattus*) propagates efficiently in human hepatoma cell lines. *Virus Res* **185**, 92–102.

Kabrane-Lazizi, Y., Meng, X. J., Purcell, R. H. & Emerson, S. U. (1999). Evidence that the genomic RNA of hepatitis E virus is capped. *J Virol* **73**, 8848–8850.

Koonin, E. V., Gorbalenya, A. E., Purdy, M. A., Rozanov, M. N., Reyes, G. R. & Bradley, D. W. (1992). Computer-assisted assignment of functional domains in the nonstructural polyprotein of hepatitis E virus: delineation of an additional group of positive-strand RNA plant and animal viruses. *Proc Natl Acad Sci U S A* **89**, 8259–8263.

Kosaka, N., Iguchi, H., Yoshioka, Y., Takeshita, F., Matsuki, Y. & Ochiya, T. (2010). Secretory mechanisms and intercellular transfer of microRNAs in living cells. *J Biol Chem* **285**, 17442–17452.

Lorenzo, F. R., Tanaka, T., Takahashi, H., Ichiyama, K., Hoshino, Y., Yamada, K., Inoue, J., Takahashi, M. & Okamoto, H. (2008). Mutational events during the primary propagation and consecutive passages of hepatitis E virus strain JE03-1760F in cell culture. *Virus Res* **137**, 86–96.

Martin-Serrano, J., Yaravoy, A., Perez-Caballero, D. & Bieniasz, P. D. (2003). Divergent retroviral late-budding domains recruit vacuolar protein sorting factors by using alternative adaptor proteins. *Proc Natl Acad Sci U S A* **100**, 12414–12419.

Meng, X. J. (2013). Zoonotic and foodborne transmission of hepatitis E virus. *Semin Liver Dis* **33**, 41–49.

Mori, Y., Koike, M., Moriishi, E., Kawabata, A., Tang, H., Oyaizu, H., Uchiyama, Y. & Yamanishi, K. (2008). Human herpesvirus-6 induces MVB formation, and virus egress occurs by an exosomal release pathway. *Traffic* **9**, 1728–1742.

Nagashima, S., Takahashi, M., Jirintai, S., Tanaka, T., Nishizawa, T., Yasuda, J. & Okamoto, H. (2011a). Tumour susceptibility gene 101 and the vacuolar protein sorting pathway are required for the release of hepatitis E virions. *J Gen Virol* **92**, 2838–2848.

Nagashima, S., Takahashi, M., Jirintai, Tanaka, T., Yamada, K., Nishizawa, T. & Okamoto, H. (2011b). A PSAP motif in the ORF3 protein of hepatitis E virus is necessary for virion release from infected cells. *J Gen Virol* **92**, 269–278.

Nagashima, S., Takahashi, M., Jirintai, S., Tanggis, Kobayashi, T., Nishizawa, T. & Okamoto, H. (2014). The membrane on the surface of hepatitis E virus particles is derived from the intracellular membrane and contains trans-Golgi network protein 2. *Arch Virol* **159**, 979–991.

Okamoto, H. (2007). Genetic variability and evolution of hepatitis E virus. *Virus Res* **127**, 216–228.

Ostrowski, M., Carmo, N. B., Krumeich, S., Fanget, I., Raposo, G., Savina, A., Moita, C. F., Schauer, K., Hume, A. N. & other authors (2010). Rab27a and Rab27b control different steps of the exosome secretion pathway. *Nat Cell Biol* **12**, 19–30, 1–13.

Purcell, R. H. & Emerson, S. U. (2008). Hepatitis E: an emerging awareness of an old disease. *J Hepatol* **48**, 494–503.

Ramakrishnaiah, V., Thumann, C., Fofana, I., Habersetzer, F., Pan, Q., de Ruiter, P. E., Willemsen, R., Demmers, J. A., Stalin Raj, V. & other authors (2013). Exosome-mediated transmission of hepatitis C virus between human hepatoma Huh7.5 cells. *Proc Natl Acad Sci U S A* **110**, 13109–13113.

Reynolds, E. S. (1963). The use of lead citrate at high pH as an electron-opaque stain in electron microscopy. *J Cell Biol* **17**, 208–212.

Takahashi, M., Hoshino, Y., Tanaka, T., Takahashi, H., Nishizawa, T. & Okamoto, H. (2008a). Production of monoclonal antibodies against hepatitis E virus capsid protein and evaluation of their neutralizing activity in a cell culture system. *Arch Virol* **153**, 657–666.

Takahashi, M., Yamada, K., Hoshino, Y., Takahashi, H., Ichiyama, K., Tanaka, T. & Okamoto, H. (2008b). Monoclonal antibodies raised against the ORF3 protein of hepatitis E virus (HEV) can capture HEV particles in culture supernatant and serum but not those in feces. *Arch Virol* **153**, 1703–1713.

Takahashi, M., Tanaka, T., Takahashi, H., Hoshino, Y., Nagashima, S., Jirintai, Mizuo, H., Yazaki, Y., Takagi, T. & other authors (2010). Hepatitis E Virus (HEV) strains in serum samples can replicate efficiently in cultured cells despite the coexistence of HEV antibodies: characterization of HEV virions in blood circulation. *J Clin Microbiol* **48**, 1112–1125.

Tam, A. W., Smith, M. M., Guerra, M. E., Huang, C. C., Bradley, D. W., Fry, K. E. & Reyes, G. R. (1991). Hepatitis E virus (HEV): molecular cloning and sequencing of the full-length viral genome. *Virology* **185**, 120–131.

Tamai, K., Tanaka, N., Nakano, T., Kakazu, E., Kondo, Y., Inoue, J., Shiina, M., Fukushima, K., Hoshino, T. & other authors (2010). Exosome secretion of dendritic cells is regulated by Hrs, an ESCRT-0 protein. *Biochem Biophys Res Commun* **399**, 384–390.

Tamai, K., Shiina, M., Tanaka, N., Nakano, T., Yamamoto, A., Kondo, Y., Kakazu, E., Inoue, J., Fukushima, K. & other authors (2012). Regulation of hepatitis C virus secretion by the Hrs-dependent exosomal pathway. *Virology* **422**, 377–385.

Tanaka, T., Takahashi, M., Kusano, E. & Okamoto, H. (2007). Development and evaluation of an efficient cell-culture system for Hepatitis E virus. *J Gen Virol* **88**, 903–911.

Tei, S., Kitajima, N., Takahashi, K. & Mishiro, S. (2003). Zoonotic transmission of hepatitis E virus from deer to human beings. *Lancet* **362**, 371–373.

Ticehurst, J. (1991). Identification and characterization of hepatitis E virus. In *Hepatitis and Liver Disease*, pp. 501–513. Edited by F. B. Hollinger, S. M. Lemon & H. Margolis. Baltimore: Williams & Wilkins.

Trajkovic, K., Hsu, C., Chiantia, S., Rajendran, L., Wenzel, D., Wieland, F., Schwille, P., Brügger, B. & Simons, M. (2008). Ceramide triggers budding of exosome vesicles into multivesicular endosomes. *Science* **319**, 1244–1247.

Wei, T., Hibino, H. & Omura, T. (2009). Release of Rice dwarf virus from insect vector cells involves secretory exosomes derived from multivesicular bodies. *Commun Integr Biol* **2**, 324–326.

Yamada, K., Takahashi, M., Hoshino, Y., Takahashi, H., Ichiyama, K., Nagashima, S., Tanaka, T. & Okamoto, H. (2009a). ORF3 protein of hepatitis E virus is essential for virion release from infected cells. *J Gen Virol* **90**, 1880–1891.

Yamada, K., Takahashi, M., Hoshino, Y., Takahashi, H., Ichiyama, K., Tanaka, T. & Okamoto, H. (2009b). Construction of an infectious cDNA clone of hepatitis E virus strain JE03-1760F that can propagate efficiently in cultured cells. *J Gen Virol* **90**, 457–462.

Yazaki, Y., Mizuo, H., Takahashi, M., Nishizawa, T., Sasaki, N., Gotanda, Y. & Okamoto, H. (2003). Sporadic acute or fulminant hepatitis E in Hokkaido, Japan, may be food-borne, as suggested by the presence of hepatitis E virus in pig liver as food. *J Gen Virol* **84**, 2351–2357.

Arch Virol (2014) 159:979–991
DOI 10.1007/s00705-013-1912-3

ORIGINAL ARTICLE

The membrane on the surface of hepatitis E virus particles is derived from the intracellular membrane and contains trans-Golgi network protein 2

Shigeo Nagashima · Masaharu Takahashi · Suljid Jirintai · Tanggis · Tominari Kobayashi · Tsutomu Nishizawa · Hiroaki Okamoto

Received: 17 May 2013 / Accepted: 28 October 2013 / Published online: 13 November 2013

Abstract Our previous studies demonstrated that hepatitis E virus (HEV) requires the multivesicular body (MVB) pathway to release virus particles, suggesting that HEV utilizes the cellular ESCRT machinery in the cytoplasm, not at the cell surface, to be released from infected cells. In this study, we generated a murine monoclonal antibody (mAb) against the membrane-associated HEV particles to examine whether the membrane is derived from intracellular vesicles or the cell surface. An established mAb, TA1708, was found to capture the membrane-associated HEV particles, but not the membrane-dissociated particles or fecal HEV, in an immunocapture RT-PCR assay. Furthermore, digitonin treatment confirmed that the membrane on the surface of cell-culture-generated HEV particles was a lipid membrane. Double immunofluorescence staining revealed that mAb TA1708 specifically recognizes trans-Golgi network protein 2 (TGOLN2), an intracellular antigen derived from the trans-Golgi network. Supporting these findings, HEV particles with lipid membranes and ORF3 proteins on their surface were found abundantly in the lysates of HEV-infected cells. These results indicate that HEV forms membrane-associated particles in the cytoplasm, most likely by budding into intracellular vesicles, and that the released HEV particles with a lipid membrane retain the antigenicity of TGOLN2 on their surface.

S. Nagashima · M. Takahashi · S. Jirintai · Tanggis · T. Kobayashi · T. Nishizawa · H. Okamoto (✉)
Division of Virology, Department of Infection and Immunity, Jichi Medical University School of Medicine, 3311-1 Yakushiji, Shimotsuke, Tochigi 329-0498, Japan
e-mail: hokamoto@jichi.ac.jp

Introduction

Hepatitis E virus (HEV), a member of the genus *Hepevirus* in the family *Hepeviridae*, is the causative agent of acute and fulminant hepatitis E, which occurs in many parts of the world, principally as a water-borne infection in developing countries and zoonotically in industrialized countries [5, 6, 9, 35, 43, 47]. HEV has a single-stranded, positive-sense RNA genome of approximately 7,200 nucleotides (nt). The genome is capped and polyadenylated [19, 40] and contains a 5' untranslated region (UTR), three open reading frames (ORFs; ORF1, ORF2 and ORF3), a 3′ UTR and a poly(A) tail at the 3′ terminus [11]. ORF1 encodes non-structural proteins, including methyltransferase, papain-like cysteine protease, helicase and RNA-dependent RNA polymerase [1, 21]. ORF2 and ORF3 overlap, and the ORF2 and ORF3 proteins are translated from a bicistronic subgenomic RNA of 2.2 kb in length [15, 17]. The ORF2 protein is the viral capsid protein, while the ORF3 protein is a small protein of only 113 or 114 amino acids (aa) that is suggested to act as an adapter to link the intracellular transduction pathways, reduce the host inflammatory response and protect virus-infected cells [5]. Recently, it was found that ORF3 proteins play an important role in virion egress from infected cells [12, 30, 45].

Four major genotypes (1-4) of HEV have been identified in humans. While HEV genotypes 1 and 2 have only been found in humans and are associated with epidemics in developing countries, HEV genotypes 3 and 4 are zoonotic and responsible for sporadic cases of disease worldwide [32]. A number of animal strains of HEV have also been identified in several animal species including chickens, pigs, wild boars, rabbits and rats [28].

HEV particles present in feces and bile are non-enveloped, while those in circulating blood and culture supernatant have been found to be covered with a cellular membrane, similar to

enveloped viruses [39]. Enveloped viruses acquire their envelope by budding through cellular membranes of different origin. HIV-1 becomes enveloped while budding through the plasma membrane, and the release of nascent virions requires a membrane fission event that separates the viral envelope from the cell surface [10]. To facilitate this crucial step in its life cycle, HIV-1 exploits the endosomal sorting complexes required for the transport (ESCRT) complexes (ESCRT-I, ESCRT-II and ESCRT-III) that constitute the cellular membrane remodeling and fission machinery known as the ESCRT pathway [14]. Other enveloped RNA viruses, such as the Ebola virus [26], avian sarcoma virus (ASV) [33] and, more recently, hepatitis C virus (HCV) [3, 7], have also been shown to utilize ESCRT complexes during virion morphogenesis. Furthermore, enveloped DNA viruses, including hepatitis B virus (HBV) [23] and herpes simplex virus 1 (HSV-1) [8], have been reported to exploit the multivesicular body (MVB) machinery.

In our previous study, we demonstrated that the PSAP motif(s) in the ORF3 protein is necessary for the egress of HEV particles from infected cells and proposed that the PSAP motifs in the ORF3 protein play a role as the functional domain required for virion release associated with lipids and the ORF3 protein [30]. Furthermore, tumor susceptibility gene 101 (Tsg101), a cellular factor involved in the budding of viruses containing the P(T/S)AP late domain and a component of ESCRT-I, and the enzymatic activity of vacuolar protein sorting-associated protein 4A (Vps4A) and VPs4B are involved in the release of HEV virions, thus suggesting that HEV utilizes the MVB machinery to exit cells [31]. However, the nature and origin of the virion membrane have not yet been characterized.

In this study, we generated a murine monoclonal antibody (mAb) against membrane-associated HEV particles using purified cell-culture-generated HEV particles as immunogens. An established mAb, TA1708, bound specifically to the component of the membrane on the surface of the HEV particles and reacted with an intracellular antigen that was found to be trans-Golgi network protein 2 (TGOLN2) in double staining immunofluorescence studies; however, it did not react with the plasma membrane. The membrane-associated HEV particles were present abundantly in lysates of infected cells. Based on the results obtained in the present study, we propose that HEV utilizes the endomembrane for membrane formation and budding and that TGOLN2 is a surface antigen of membrane-associated HEV particles.

Materials and methods

Cell culture

PLC/PRF/5 cells (ATCC no. CRL-8024) were grown in Dulbecco's modified Eagle's medium (DMEM) containing 10 % (vol/vol) heat-inactivated fetal calf serum (FCS), 100 U/ml of penicillin, 100 μg/ml of streptomycin and 2.5 μg/ml of amphotericin B (growth medium) at 37 °C in a humidified 5 % CO_2 atmosphere, as described previously [42].

Viruses

A fecal suspension containing a wild-type genotype 3 HEV (JE03-1760F strain; 2.0×10^7 copies/ml) [36] and a culture supernatant containing a cell-culture-generated JE03-1760F variant (1.2×10^8 copies/ml) [24] were used as reference viruses in this study. HEV progenies in the culture supernatant of PLC/PRF/5 cells transfected with RNA transcripts of an infectious HEV cDNA clone (pJE03-1760F/wt, GenBank accession no. AB437316) and its derivative ORF3-deficient mutant (pJE03-1760F/ΔORF3, GenBank accession no. AB437317), whose initiation codon of the ORF3 gene was mutated to GCA (Ala), were used for the experiments [46].

Preparation of membrane-associated HEV particles as immunogens

The cell-culture-adapted JE03-1760F strain in the 23rd generation of supernatant passage (JE03-1760F_p23) [24] was cultivated in PLC/PRF/5 cells in a 75-cm^2 culture bottle (Asahi Glass Co. Ltd., Tokyo, Japan) with growth medium for more than 120 days, and culture media (204 ml) harvested during days 34-102 were pooled. The pooled culture media were spun down in a Beckman SW28 rotor (Beckman Coulter, Inc., Indianapolis, IN) at 112,700 × g at 10 °C for 5 h. The resulting pellets were suspended in 2 ml of TEN buffer containing 0.01 M Tris-HCl (pH 7.5), 0.001 M EDTA and 0.1 NaCl and subjected to sucrose density gradient ultracentrifugation as described previously [38]. A 2-ml volume of pooled peak fractions at a sucrose density of 1.14 g/ml was used as a viral suspension for immunization.

Production of mAbs

mAbs were raised against purified cell-culture-generated HEV particles using a method described elsewhere [44], with slight modifications. Briefly, BALB/c mice were injected three times intraperitoneally with 100 or 150 μl of the viral suspension (1.3×10^{10} copies/ml) in PBS on days 0, 14 and 53 and with 0.1 μg of inactivated pertussis toxin (Pertussis Toxin Salt-Free; List Biological Laboratories, Inc., Campbell, CA) on day 161 as an adjuvant, followed by the intravenous injection of 75 μl of the same viral suspension (with the adjuvant) on day 192, three days before fusion. NS-1 myeloma cells were fused with

immunized spleen cells at a ratio of 1:10. The screening of mAbs was performed using immunocapture RT-PCR as described below. Hybridomas secreting mAbs against membrane-associated HEV particles of the desired specificity were propagated in the peritoneal cavities of mice that had been made ascitic due to the injection of 2,6,10,14-tetramethylpentadecane. The ascites fluid was harvested approximately 10 days after implantation, and the γ-globulin fractions were precipitated with 2 M $(NH_4)_2SO_4$ and then purified via gel filtration in Sephadex G-200 (GE Healthcare UK Ltd., Buckinghamshire, England). The mAbs were tested for their immunoglobulin class/subclass using a murine monoclonal antibody isotyping kit (Bio-Rad Laboratories, Hercules, CA).

Immunocapture RT-PCR assay

To screen mAbs with virus-binding ability, immunocapture RT-PCR was performed as described previously [38] with the following modifications. In brief, the wells of the immunoplate (part no. 762071; Greiner Bio-One GmbH, Frickenhausen, Germany) were washed with saline three times, and 50 μl each of 10 μg/ml goat affinity-purified antibody to murine IgG (#55479; MP Biomedicals, Santa Ana, CA) and mouse IgM (#55484; MP Biomedicals) in saline was added to each well and immobilized. The wells were incubated at room temperature overnight and then washed five times with saline. Fifty microliters of culture supernatant containing mAbs was added to each well and incubated with shaking at room temperature for 1.5 h. The solution in each well was removed, and the wells were washed three times with saline. Fifty microliters of diluted culture supernatant containing HEV progeny (approximately 10^5 copies/ml) was added to each well and incubated with shaking at room temperature for 2 h and then incubated with shaking at 4 °C overnight. The solution in each well was removed, and the wells were washed three times with saline. One hundred fifty microliters of TRIzol® LS Reagent (Invitrogen, Carlsbad, CA) and 50 μl of distilled water were directly added twice to each well. The RNA was then extracted and subjected to quantitative detection of HEV RNA as described below.

To evaluate the specificity of the established mAbs and further characterize the HEV particles, an immunocapture RT-PCR assay was also performed, with or without prior treatment of HEV particles with 0.1 % (vol/vol) sodium deoxycholate and/or 0.1 % (wt/vol) trypsin at 37 °C for 2 h, or 1.5 % (wt/vol) digitonin (Nacalai Teaque, Kyoto, Japan) at room temperature for 13 h. In addition to the mAb (TA1708) against membrane-associated HEV particles generated in the present study, an anti-ORF2 mAb (H6225) [37] and an anti-ORF3 mAb (TA0536) [38] were used.

Quantitation of HEV RNA

RNA extraction was performed using TRIzol® LS Reagent (Invitrogen). Quantification of HEV RNA was performed by real-time RT-PCR using a LightCycler apparatus (Roche Diagnostics, Mannheim, Germany), with a QuantiTect Probe RT-PCR Kit (QIAGEN, Hilden, Germany), primer set, and a probe targeting the ORF2 and ORF3 overlapping region, as described previously [37].

Digitonin treatment and sucrose density gradient centrifugation

The culture supernatants containing HEV progeny (1.0×10^6 copies), collected from PLC/PRF/5 cells transfected with RNA transcripts of pJE03-1760F/wt or pJE03-1760F/ΔORF3 at 18 days post-transfection, were treated with or without 1.5 % digitonin at room temperature for 13 h. The digitonin-treated culture supernatants were subjected to equilibrium centrifugation in a sucrose density gradient as described previously [38]. The gradients were fractionated, and the density of each fraction was measured using refractometry. Similarly, the culture supernatant containing 6.0×10^6 copies of HEV or cell lysates containing 5.0×10^7 copies of HEV collected from the PLC/PRF/5 cells transfected with RNA transcripts of pJE03-1760F/wt at 28 days post-transfection were subjected to equilibrium centrifugation in a sucrose density gradient.

Immunofluorescence assay

PLC/PRF/5 cells in a 4-well chamber slide (Nunc, Roskilde, Denmark) were subjected to immunofluorescence staining using mAb TA1708 and rabbit polyclonal antibodies raised against well-established cellular markers (see below) as the primary antibodies, followed by Alexa Fluor 488–conjugated anti-mouse IgM (Molecular Probes, Eugene, OR) and Alexa Fluor 594–conjugated anti-rabbit IgG (Molecular Probes) as the secondary antibodies. For staining of Myc-tagged TGOLN2 recombinant protein in the cells transfected with expression plasmid (see below), anti-Myc mAb (9E10; Santa Cruz Biotechnology) labeled by using a Zenon Alexa Fluor 488 mouse IgG labelling kit (Molecular Probes) as well as mAb TA1708 as the primary antibody and Alexa Fluor 568–conjugated anti-mouse IgM (Molecular Probes) as the secondary antibody, or anti-TGOLN2 antibody (HPA012723; Sigma-Aldrich, St Louis, Mo) as the primary antibody and Alexa Fluor 594–conjugated anti-rabbit IgG (Molecular Probes) as the secondary antibody, were used. Briefly, the cultured cells were fixed in 4 % (vol/vol) paraformaldehyde (Wako Pure Chemical Industries, Ltd., Osaka, Japan) at room temperature for

15 min and treated with 50 mM glycine in phosphate-buffered saline (PBS) at room temperature for 30 min. The cells were treated with cold methanol at −20 °C for 15 min and permeabilized in PBS containing 0.2 % (vol/vol) Triton X-100 at room temperature for 15 min. Nonspecific binding was blocked with 1 % BSA in PBS at room temperature for 30 min. The fixed cells were incubated with the appropriate primary antibodies diluted in PBS containing 1 % BSA and 0.1 % Triton X-100 or Can Get Signal® immunostain solution A or B (Toyobo, Osaka, Japan) at 4 °C overnight. The rabbit polyclonal antibodies used as the primary antibodies were as follows: Golgi marker (giantin, sc-67168; Santa Cruz Biotechnology, Santa Cruz, CA), trans-Golgi network (TGN) markers including TGN46 (T7576; Sigma-Aldrich), TGN38 (sc-33783; Santa Cruz Biotechnology), syntaxin 6 (#2869; Cell Signaling technology, Beverly, MA) and TGOLN2, MVB marker (CD63, sc-15363; Santa Cruz Biotechnology), early endosomal marker (EEA1, E3906; sigma-aldrich), late endosomal marker (Rab7, sc-10767; Santa Cruz Biotechnology) and recycling endosomal marker (Rab11, #3539; Cell Signaling technology). After washing with PBS, the cells were stained with appropriate secondary antibodies diluted in PBS containing 1 % BSA and 0.1 % Triton X-100 or Can Get Signal® immunostain solution A or B (Toyobo) at room temperature for 2 h. The nuclei were counterstained with 4′,6-diamidino-2-phenylindole (DAPI; Roche Diagnostics, Mannheim, Germany). The slide glasses were mounted with Fluoromount/Plus (Diagnostic BioSystems, Pleasanton, CA) and then viewed under a FV1000 confocal laser microscope (Olympus, Tokyo, Japan). For the quantitation of co-localization in cells (mean ± standard error), at least 20 cells each were used for calculations in two independent experiments.

Expression of TGOLN2 recombinant protein

The expression plasmid for FLAG- and Myc-tagged TGOLN2 (pFLAG-Myc-CMV-22-TGOLN2) was constructed as follows. The coding sequence of TGOLN2 gene was amplified by PCR using a human cDNA clone of TGOLN2 (FCC138E05; Toyobo) as a template, *TaKaRa Ex Taq*® DNA polymerase (TaKaRa Bio, Otsu, Japan), and appropriate oligonucleotide primers. The sequences of the primers used were as follows: TGOLN2-EcoRI-A-335 P, 5′-TGAATTCAATGCGGTTCGTGGTTGCCTTGG-3′; *Eco*RI site (underlined) and plus-strand sequence (nt 335-356) of TGOLN2 gene, and TGOLN2-XbaI-1645 M, 5′-ATCTAGAGGACTTCTGGTCCAAACGTTGG-3′; *Xba*I site (underlined) and minus-strand sequence (nt 1624-1645) of TGOLN2 gene. The PCR product was subcloned into the T-vector pMD20 (TaKaRa Bio), and the nucleotide sequence between the *Eco*RI and *Xba*I sites of the derived clone was confirmed. The *Eco*RI-*Xba*I fragment of this subclone was ligated into pFLAG-Myc-CMV-22 (Sigma-Aldrich), from which the *Eco*RI-*Xba*I fragment had been removed, yielding pFLAG-Myc-CMV-22-TGOLN2.

PLC/PRF/5 cells in a four-well chamber slide (Nunc) were transfected with 0.5 μg of pFLAG-Myc-CMV-22-TGOLN2 using TransIT-LT1 reagent (Mirus Bio, Madison, WI) according to the manufacturer's recommendations. The empty vector was used as negative control. At 48 h after transfection, an immunofluorescence assay was performed to investigate the co-localization between the TGOLN2 recombinant protein and the antigen recognized by mAb TA1708, as described above.

Results

Production and characterization of mAbs

Six hybridoma clones secreting mAbs designated as TA1703, TA1705, TA1706, TA1707, TA1708 and TA1709 against the cell-culture-generated HEV particles were obtained in the present study. The specificity of these six mAbs was verified using immunocapture RT-PCR. Among them, mAb TA1708 (IgM class) exhibited the highest reactivity with viral particles associated with a membrane in the culture supernatant. Thereafter, mAb TA1708 was used in the further analyses. The membrane-associated HEV particles were efficiently captured by mAb TA1708 (86.8 %) (Table 1). In contrast, almost none of the viruses were captured by anti-ORF2 (H6225) or anti-ORF3 (TA0536) mAbs (5.3 % and 7.1 %, respectively). As with fecal HEV, no viruses were captured by mAb TA1708 (0.1 %). On the other hand, the viruses in feces that are known to be non-enveloped were efficiently trapped by the anti-ORF2 mAb (92.3 %) but not by the anti-ORF3 mAb (0.0 %). These results suggest that mAb TA1708 binds to membrane-associated HEV particles.

mAb TA1708 binds specifically to the membrane on the surface of HEV particles

To examine further whether mAb TA1708 binds to the membrane on the surface of viral particles, an immunocapture RT-PCR assay was performed using mAb TA1708, anti-ORF2 (H6225), and anti-ORF3 (TA0536) mAbs with or without prior treatment with detergents (Table 1). Consistent with our previous observations [39], when the particles in the culture supernatant were treated with 0.1 % or 1 % sodium deoxycholate, the efficiency of binding of HEV particles induced by anti-ORF2 mAb increased to 80.9 % and 84.2 %, respectively, while that induced by

Table 1 Reactivity of mAb TA1708 with HEV particles with or without prior treatment with detergents, as evaluated using immunocapture RT-PCR

Virus[a]	% of captured HEV in the total HEV per well		
	mAb TA1708	mAb H6225 (anti-ORF2)	mAb TA0536 (anti-ORF3)
Without pre-treatment with detergent			
Culture supernatant	86.8	5.3	7.1
Fecal supernatant	0.1	92.3	0.0
With pre-treatment with detergents[b]			
Culture supernatant			
0.1 % DOC-Na	14.6	80.9	59.0
1 % DOC-Na	11.2	84.2	44.3
0.1 % DOC-Na and 0.1 % trypsin	3.5	92.4	0.4
1 % DOC-Na and 0.1 % trypsin	0.8	94.1	0.2
0.1 % trypsin	73.5	7.1	0.2

[a] Viruses derived from the culture supernatant of infected cells (strain JE03-1760F) were subjected to immunocapture RT-PCR

[b] Prior to performing the immunocapture RT-PCR assay, the viruses were mixed with detergents, incubated at 37 °C for 2 hours, and then diluted 1:10 with PBS containing 0.1 % BSA

anti-ORF3 mAb increased to 59.0 % and 44.3 %, respectively. Furthermore, the binding efficiencies of HEV particles subjected to prior treatment with 0.1 % sodium deoxycholate and 0.1 % trypsin or 1 % sodium deoxycholate and 0.1 % trypsin increased to 92.4 % and 94.1 %, respectively, for the anti-ORF2 mAb and decreased to 0.4 % and 0.2 %, respectively, for the anti-ORF3 mAb. On the other hand, after treatment with these detergents or detergents/proteases, the binding efficiency of the viruses was reduced to 0.8-14.6 % for mAb TA1708 (Table 1). The virus particles in the culture supernatant treated with 0.1 % trypsin were efficiently captured by mAb TA1708 (73.5 %) but not by anti-ORF2 or anti-ORF3 mAbs (7.1 % and 0.2 %, respectively). These results indicate that mAb TA1708 binds specifically to a component of the membrane on the surface of HEV particles.

The membrane on the surface of HEV particles released into the culture supernatant is a lipid membrane

The HEV particles in the culture supernatant of the wild-type RNA- and ORF3-null mutant (ΔORF3) RNA-transfected cells were processed using digitonin, which effectively water-solubilizes lipids and has several membrane-related applications, including solubilizing membrane proteins and permeabilizing cell membranes, and changes in reactivity to mAb TA1708 were analyzed. After treatment with 1.5 % digitonin, the HEV particles were subjected to equilibrium centrifugation in a sucrose density gradient (Fig. 1). In agreement with the finding of our previous study [30], the wild-type HEV in the culture supernatant exhibited a peak density of 1.16 g/ml, while the ΔORF3 viruses in the culture supernatant banded at 1.27 g/ml in sucrose. The observed differences in buoyant density were found to be ascribable to the acquisition of the ORF3 protein and cellular membrane on the surface of the virions [38, 45]. The peak density of digitonin-treated virus particles in the culture supernatant of the wild-type RNA transfected cells shifted to 1.20 g/ml, a value that is between those observed for the membrane-associated HEV particles (1.16 g/ml) and the membrane-unassociated HEV particles (1.27 g/ml) (Fig. 1). On the other hand, the ΔORF3 mutant viruses in the culture supernatant banded at 1.27 g/ml, similar to fecal HEV, regardless of digitonin treatment.

To characterize the virus particles treated with digitonin that shifted to a peak density of 1.20 g/ml, an immunocapture RT-PCR assay was performed using anti-ORF2, ORF3 and TA1708 mAbs (Table 2). The membrane-associated particles (1.16 g/ml) in the culture supernatant of cells transfected with wild-type RNA were efficiently captured by mAb TA1708 (57.2 %), but not by the anti-

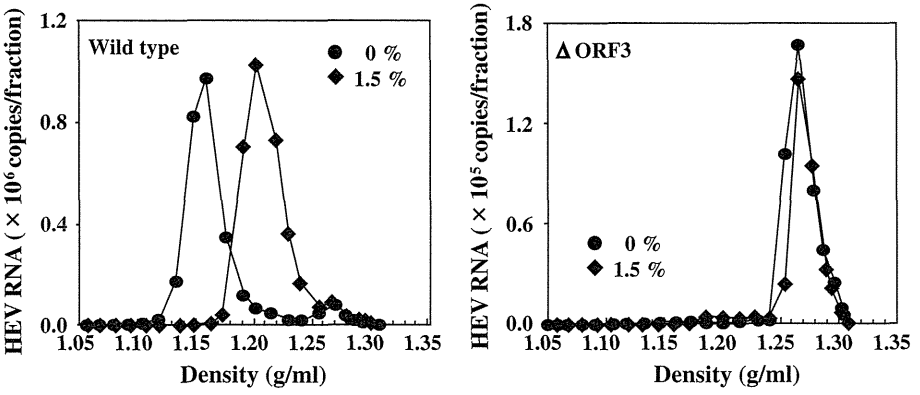

Fig. 1 Sucrose density gradient fractionation of HEV in the culture supernatants of RNA-transfected PLC/PRF/5 cells (wild-type and ΔORF3) with or without prior treatment with 1.5 % digitonin

Table 2 Reactivity of mAb TA1708 with membrane-associated and -unassociated HEV particles with or without prior treatment with 1.5% digitonin, as evaluated using immunocapture RT-PCR

Virus[a]	% of captured HEV in the total HEV per well		
	mAb TA1708	mAb H6225 (anti-ORF2)	mAb TA0536 (anti-ORF3)
pJE03-1760F/wt			
Without pre-treatment with digitonin (1.16 g/ml)	57.2	4.7	9.0
With pre-treatment with digitonin[b] (1.20 g/ml)	9.1	30.5	56.7
ΔORF3			
Without pre-treatment with digitonin (1.27 g/ml)	2.2	91.9	3.0
With pre-treatment with digitonin[b] (1.27 g/ml)	1.8	94.2	0.8

[a] Viruses were derived from the culture supernatants of transfected cells (pJE03-1760F/wt or ΔORF3) at 18 days post-transfection

[b] Prior to performing the sucrose density gradient centrifugation, the viruses were mixed with 1.5% digitonin and incubated at room temperature for 13 hours

ORF2 or anti-ORF3 mAb (4.7 % and 9.0 %, respectively). In contrast, the higher-density particles (1.20 g/ml) derived from digitonin treatment in the supernatant of the wild-type virus were trapped by both anti-ORF2 and anti-ORF3 mAbs (30.5 % and 56.7 %, respectively), while the efficiency of capture by mAb TA1708 was reduced to 9.1 % (Table 2). Viral particles with or without prior treatment with 1.5 % digitonin in the culture supernatant of the cells transfected with ΔORF3 RNA were efficiently captured by the anti-ORF2 mAb (94.2 % and 91.9 %, respectively), but not by the anti-ORF3 (0.8 % and 3.0 %, respectively) or TA1708 (1.8 % and 2.2 %, respectively) mAbs. These results indicate that the membrane on the surface of the viral particles generated in the culture supernatant is a lipid membrane.

Subcellular localization of the antigen recognized by mAb TA1708

We subsequently examined the subcellular localization of the antigen recognized by mAb TA1708 using immunofluorescence confocal microscopy. PLC/PRF/5 cells were prepared on a chamber slide and stained with mAb TA1708 and Alexa Fluor 488–conjugated anti-mouse IgM. Specific signals were observed only in the cytoplasm, primarily on the fringe and unevenly in the nucleus (Fig. 2, upper panel). In contrast, no specific signals were observed in the cells stained only with Alexa Fluor 488–conjugated anti-mouse IgM (Fig. 2, lower panel). These

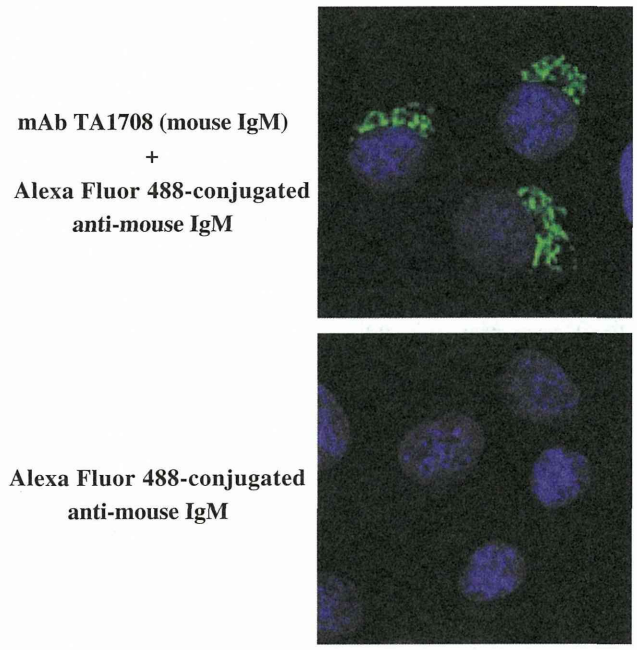

Fig. 2 Subcellular localization of the antigen recognized by mAb TA1708. PLC/PRF/5 cells were fixed and stained with mAb TA1708 and then labeled with Alexa Fluor 488–conjugated anti-mouse IgM. The nuclei were stained with DAPI. All images are representative of two independent experiments

results indicate that mAb TA1708 reacts with intracellular antigens but not with the plasma membrane, suggesting that HEV forms membrane-associated particles in the cytoplasm, likely by utilizing the membranes of intracellular vesicles.

In order to identify the antigen recognized by mAb TA1708, we carried out double staining immunofluorescence assays using antibodies against well-established cellular markers (see Materials and methods). Although the antigen recognized by mAb TA1708 was co-localized with giantin and TGN46, strong co-localization was observed with TGN46 (Fig. 3). On the other hand, no clear co-localization was observed with the other cellular markers. Using anti-TGN38 and anti-syntaxin 6 antibodies, which are antibodies against TGN marker proteins, we performed double staining with mAb TA1708. The antigen recognized by mAb TA1708 exhibited a more distinct, pronounced co-localization signal between TGN38 and TGN46 when compared with syntaxin 6 (Fig. 4A). These results suggest that mAb TA1708 recognizes TGOLN2, which is encoded by the TGOLN2 gene and is also known as TGN38, TGN46, TGN48, TGN51 or TTGN2 [20, 25, 34]. Furthermore, we carried out double staining immunofluorescence studies using an anti-TGOLN2 antibody. The antigen recognized by mAb TA1708 also demonstrated co-localization in the double staining with TGOLN2 (Fig. 4B). These results suggest that TGOLN2 derived from TGN is a surface antigen of membrane-associated HEV particles.

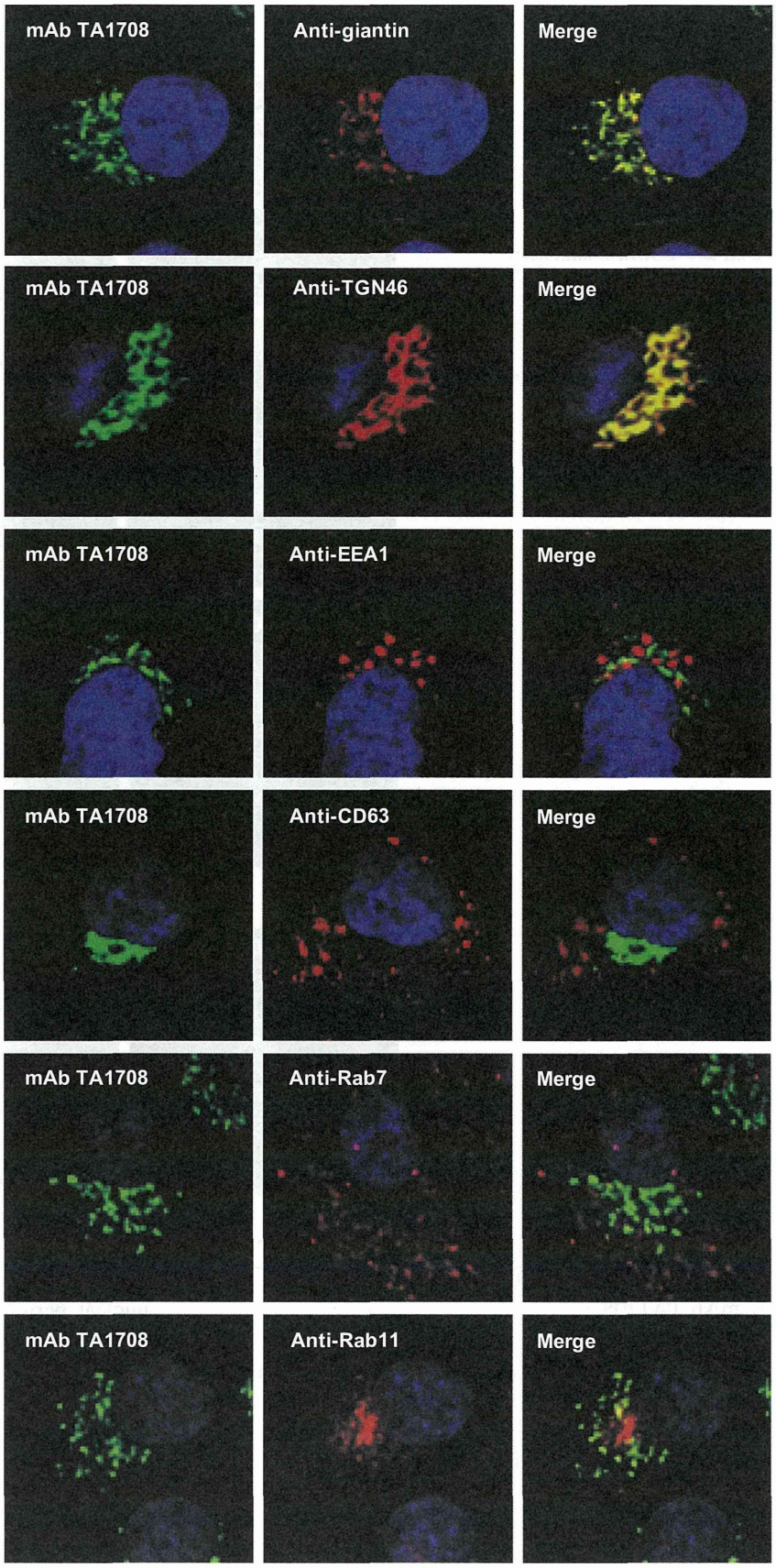

Fig. 3 Co-localization of the antigen recognized by mAb TA1708 with six established cellular markers. PLC/PRF/5 cells were fixed and double-stained with mAb TA1708 labeled with Alexa Fluor 488 and rabbit anti-giantin, anti-TGN46, anti-EEA1, anti-CD63, anti-Rab7, or anti-Rab11 antibodies labeled with Alexa Fluor 594. The nuclei were stained with DAPI. Co-localization is indicated by yellow staining. All images are representative of two independent experiments